

THE SEQUESTRATION OF CO₂ BY CONVERSION TO HYDROCARBONS

Raha Moossavi Jazari

Department of Chemistry and Biomolecular Sciences

Macquarie University

Thesis submitted for completion of the degree of Masters of Research

(MRes)

10/10/2014

Supervisor: Dr. Christopher R. McRae

Contents

Acknowledgements.....	iv
Abbreviation List.....	v
List of Tables.....	vi
List of Figures.....	vii
Abstract.....	1
Chapter 1: Introduction.....	2
1.1 History of CO ₂ and its conversion.....	2
1.2 Conventional approaches to CO ₂ to CH ₄ conversion.....	3
1.3 Problems faced regarding conventional approaches.....	5
1.4 Alternate approaches to the conversion of CO ₂ to CH ₄	6
1.5 Considerations for the silane reducing reagents being used.....	8
1.6 Proposed Project.....	9
1.7 Summary of Methodologies.....	10
Chapter 2: Experimental.....	11
2.1 Materials.....	11
2.2 Equipment and Instrumentation.....	11
2.2.1 Real-time MS.....	11
2.2.2 GC-MS.....	13
2.2.3 GC-TCD.....	15
2.2.4 FTIR.....	16
2.2.5 NMR.....	17
2.2.6 Data Processing.....	17
2.3 Synthetic Procedures and Characterisation.....	17
2.3.1 B(C ₆ F ₅) ₃ characterisation.....	17
2.3.2 Synthesis of the tandem catalyst ¹²	18
2.3.3 Synthesis of Siloxane reagents.....	19
2.3.3.1 Synthesis of ethoxytrimethylsilane mixture ²²	19
2.3.3.2 Synthesis of hexaethyldisiloxane ¹⁵	19
2.3.4 Nickel Zeolite Catalysts ^{5, 23}	20
2.3.5 Silane stock solutions.....	20
2.4 Reaction gas mixture composition.....	21
2.5 Data Acquisition.....	21
2.6 Siloxane to Silane reductions.....	21

2.6.1 H-Cube Reductions	21
2.6.2 Photochemical Reductions	22
2.6.3 Electrochemical Reductions	23
2.7 Final Flow Chart: Chronological Review of Experimental Approach	25
Chapter 3: Results and Discussion.....	26
3.1 Development of Apparatus	26
3.1.1 Production of Quantitative Gas mixtures.....	26
3.1.1.1 Volumetric gas mixing manifold	26
3.1.1.2 Partial pressure gas mixing manifold.....	27
3.1.2 Reactor design.....	29
3.2 Reaction Product analysis	31
3.2.1 Online MS.....	31
3.2.2 GC-TCD.....	36
3.2.3 FTIR.....	41
3.3 Regeneration of Silane: Evaluation of Siloxane to Silane Reduction Strategies.....	43
3.3.1 Reduction over metal catalysts	43
3.3.2 Photochemical Reductions.....	44
3.3.3 Electrochemical Reductions	45
3.4 Future Directions	49
Chapter 4: Conclusions	51
References.....	52
Appendix.....	54

Declaration of Originality

I hereby declare that the work being presented is entirely mine and has not been submitted in part or in full to any other university or institution for any other reward.

Raha Moossavi Jazari

Date: 10/10/2014

Acknowledgements

I would firstly like to thank all students and staff here within the Department of Chemistry and Biomolecular Sciences at Macquarie University. I would like to thank the Masters of Research Committee; A/Prof. Bridget Mabbutt, Dr. Louise Brown, A/Prof. Andrew Try and A/Prof. Mark Molloy. Thank you for your continuous support, motivating words and timely organisational skills.

I would especially like to thank my wonderful supervisor, Dr. Christopher McRae. Thank you for your kind assistance, continuous support (even through late nights in the lab!), patience and advice. Your teachings in the understanding and engineering behind various analytical instruments, (their maintenance, troubleshooting and development) has only made my interest towards instrumental design grow even further. Furthermore, I will always remember your first teaching by quoting your father who said, "It is a poor tradesman who blames his tools". From that moment I learnt that there is always a solution to any given problem. All you need to do is take a step back, look at the whole picture and then work through step by step, in order of gaining greater ground and piecing together a puzzle which within any given instantaneous moment seems endless, but can be considered only an illusion of time itself...

I would also like to thank my fellow colleagues within the McRae research team: Sahar Farzadnia, Zahra Khamseh Safa, Ike Li and Yvonne Yin. Thank you for welcoming me into this research group with open arms. I would also like to acknowledge the significant input and kind assistance provided by all academics within the Department, specifically Dr. Fei Liu, Dr. Ian Jamie and Dr. Danny Wong. I would also like to extend my gratitude to Anthony Gurlica.

To my dearest friends within the Department (especially within Team Manganese)... I have learnt so much from each and everyone one of you, and will cherish all our wonderful experiences together. ☺ Thank you to Ryan Kenny and Harold Spedding for supporting me and providing me their expertise behind Organic Chemistry and the principles of NMR instrumentation and analysis. I would also like to extend my appreciation to my dearest friend (...and twin sister) Yvonne Yin. I am so lucky and grateful to have sat next to you during the first year organic chemistry lecture. Thank you for listening to me, advising me, crying and laughing with me over the last five years.

Most importantly, I would like to thank my family. Your continuous love, affection and support have ultimately allowed me to see the world and all its beautiful possessions in a whole new light. I will forever be grateful. And to my lovely mother, I will always remember your teachings and experiences in life and forever hold them close to my heart. Thank you for being patient, understanding, loving, caring and embodying a best friend, sister and mother all in one. I will always remember your saying, "The keys to success are independence and love. If you genuinely love what you do and what you want to achieve in life, there is nothing that can stop you from doing so".

I would like to finish my acknowledgements to He who is one and only. I will always be forever grateful for everything I have already received and achieved, and believe that through Your guidance I can achieve even greater. I conclude this acknowledgement in the name of God.

Abbreviation List

Chemicals / Gases

Ar	Argon
B(C ₆ F ₅) ₃	Tris(pentafluorophenyl)borane
CHCl ₃	Chloroform
CDCl ₃	Chloroform-d
CH ₄	Methane
CO ₂	Carbon dioxide
CO	Carbon monoxide
DCM	Dichloromethane
H ₂	Hydrogen gas
LiAlH ₄	Lithium aluminium hydride
N ₂	Nitrogen gas
PTFE	Polytetrafluoroethylene
TC	Tandem catalyst
THF	Tetrahydrofuran

Instrumentation & Data Acquisition

ATR	Attenuated Total Reflectance
DI	Direct Injection
DRIFT	Diffuse Reflectance Infrared Fourier Transform
EI	Electron Ionisation
FTIR	Fourier Transform Infrared
GC-MS	Gas Chromatography-Mass Spectrometry
GC-TCD	Gas Chromatography-Thermal Conductivity Detector
IR	Infrared
MS	Mass Spectrometry
MFC	Mass Flow Controller
NMR	Nuclear Magnetic Resonance
TEM	Transmission electron microscopy
XRD	Xray Diffraction

Units

Å	Angstrom
amu	Atomic Mass Unit
atm	Atmospheres
cm	Centimetres
ID	Internal diameter
m	Metres
mbar	Millibar
MHz	Megahertz
min	Minutes
mol	Moles
mol %	Mole percentage
mV	Millivolts
[m/z(%)]	Mass to charge ratio, relative peak intensity to base peak
OD	Outer diameter
psia	Pounds per square inch absolute
psig	Pounds per square inch gauge

rpm	Rotations per minute
s	Seconds
sccm	standard cubic centimetres per minute
sig. figs	Significant Figures
°C	Degrees Celsius

Other Terms

FLPs	Frustrated Lewis Pairs
------	------------------------

List of Tables

Table 1. Operating conditions of MS used for two method files.....	12
Table 2. The MCD matrix set up taken from the gas calibration values obtained during standard runs. Note that no direct relationship can be established between the calibration factors used to analyse samples at 15 and 29 psig, as different interface lines were used for each calibration.	13
Table 3. Instrumental conditions for GC-MS used for two separate method files.	14
Table 4. Operating conditions of the GC-TCD method file used.	15
Table 5. The experimental sample matrix for 15.00 psig.	16
Table 6. The experimental sample matrix for 29.00 psig.	16
Table 7. Instrumental conditions and parameters used for ATR and DRIFT spectroscopic modes.	17
Table 8. Stock solutions made using the silane reducing reagent, CHCl ₃ and dodecane.	20
Table 9. Composition of the gas mixtures used for the methanation reactions.	21
Table 10. Instrumental parameters and conditions set on the H-cube for reductions.	22
Table 11. The Potentiostat instrumental parameters and conditions set for the electrochemical reduction system.	24
Table 12. A summarised table for calculating the rate constants and respective 95 % confidence intervals for the samples measured at a pressure of 15 psig.	36
Table 13. The relative mol % of methane calculated at 15 psig using the percentage area of each gas component and interpolating from the regression plot shown in Figure 17.	38
Table 14. The relative mol % of methane calculated at 29 psig using the percentage area of each gas component and interpolating from the regression plot shown in Figure 17.	39
Table 15. Comparison of the calculated rate constants and percentage yield of CH ₄ determined at 15 psig using real-time MS and GC-TCD measurements.	40

List of Figures

Figure 1. The process involved for the conversion of CO ₂ . As a minimal requirement, CO ₂ and a high energy reducing reagent are required in addition to a catalyst, which will provide an alternative pathway for the reaction to progress to completion using a smaller activation energy, in order of reducing the C=O bond to a C-H bond ⁸	4
Figure 2. Heterolytic cleavage of H ₂ by amines and B(C ₆ F ₅) ₃ . The thermal dissociation of the B-N bond, resulting in a Lewis-acid Lewis-base adduct ¹²	7
Figure 3. Activation of CO ₂ by the FLP under relatively mild conditions redrawn from ¹³	7
Figure 4. Glass cell experimental setup for electrochemical reduction of siloxanes.....	24
Figure 5. Experimental approach implemented during the project.	25
Figure 6. Schematic diagram for the manifold used for the volumetric method of gas mixtures.	26
Figure 7. Schematic diagram for the manifold used for the partial pressure method of gas mixture production.....	28
Figure 8. Reactor Design 1	29
Figure 9. Reactor Design 2	30
Figure 10. Connections made to the reaction vessel.....	31
Figure 11. Real time methane concentration trace, as reported by the MS, produced from the reaction of diethyl silane/B(C ₆ F ₅) ₃ +TC with 30 mol% CO ₂ at 15 psig. Data shown is from 60 s onwards. Prior to 60 s the signal from the MS is unreliable due to fluctuating pressure changes as flows stabilise.	32
Figure 12. Data from Figure 11 after modelling using Equation 2.....	33
Figure 13. Modelled real time methane concentration trace, as reported by the MS, produced from the reaction of diethyl silane/B(C ₆ F ₅) ₃ + tandem catalyst (S009) with 30 mol% CO ₂ at 15 psig. The data is shown from 60 s onwards. Prior to 60 s the signal from MS is unreliable due to fluctuating pressure changes as flows stabilise.....	34
Figure 14. Plot of ln([CH ₄] _{max} - [CH ₄] _t) against time demonstrating a linear relationship between the two parameters, thus establishing a pseudo first order reaction.	35
Figure 15. Plot of 1/([CH ₄] _{max} - [CH ₄] _t) against time demonstrating a non-linear relationship and therefore does not follow a second order reaction.	35
Figure 16. An example of a chromatogram obtained during a sample run using the GC-TCD.	37
Figure 17. Regression plot for methane calibration showing area % of the methane with respect to the internal standard against the relative percentage of CH ₄	38
Figure 18. Stacked IR spectra of reaction samples using n-butylsilane at 15 psig.....	42

Figure 19. GC-MS chromatograms of the pre and post H-cube reductions depicting no new peaks being observed.	44
Figure 20. Chromatogram with stacked peaks for pre and post photoreduction samples using the hexadiethylsiloxanes synthesised with heptanoic acid.	45
Figure 21. Cyclic voltammogram of a blank sample solution containing THF, tandem catalyst and tetrabutylammonium perchlorate (supporting electrolyte).	46
Figure 22. Cyclic voltammogram of a reaction sample solution containing THF, tandem catalyst and tetrabutylammonium perchlorate (supporting electrolyte) and the hexaethylsiloxane synthesised using heptanoic acid.	47
Figure 23. Stacked IR spectra of the pre and post electrochemical reductions.	48

Abstract

Carbon dioxide (CO₂) is an abundant greenhouse gas continually emitted into the atmosphere from both natural sources and anthropogenic sources including: fossil fuel combustion, fracking techniques, industrial materials production and land deforestation. Consequently, the natural carbon cycle is overridden leading to strong debates regarding global warming and climate change.

The reduction of CO₂ to methane (CH₄), a process known as methanation, has been the subject of extensive study. However most approaches suffer from limitations including: use of sacrificial and expensive metal-based catalysts, high temperature and pressure requirements leading to incomplete reactions, resulting in CO and unreacted CO₂ products. Alternative approaches currently being suggested involve use of silane-based reducing reagents with Lewis acid type catalysts.

Consequently this project focused on screening four silane-based reducing agents against B(C₆F₅)₃, a B(C₆F₅)₃/hindered amine tandem catalyst and B(C₆F₅)₃ + tandem catalyst to determine efficiencies of CH₄ formation and rates of reactions. Additionally, the continuous in situ regeneration of siloxane byproducts into silane reducing reagents was investigated.

The conversion of CO₂ to CH₄ holds significant potential for the chemical capture of CO₂ and storage of hydrogen in the form of CH₄ which has many applications including: commercial power stations, petrochemical refining and natural gas.

Chapter 1: Introduction

1.1 History of CO₂ and its conversion

Carbon dioxide (CO₂) is a greenhouse gas that is being continually emitted into the atmosphere, with reported global CO₂ emissions reaching 34.5 billion tonnes in 2012¹. The significant accumulation rate of this gas is primarily due to human-dependent activities such as combustion of fossil fuels (such as natural gas, coal and petroleum) and fracking techniques. Further sources of CO₂ include atmospheric CO₂ produced by industrial non-combustion sources including construction activities (cement and steel production) and land deforestation¹⁻². The release of CO₂ into the atmosphere through human and non-human sources has significantly increased, to the point where natural resources including plants are unable to remove enough CO₂ at a proportional rate, causing great concerns with regards to global warming and climate change.

However with its vast abundance as a waste product, CO₂ is currently being utilised for a variety of chemical synthetic applications including its conversion into a wide spectrum of compounds of higher practicality; hydrocarbons, methanol, polycarbonates, urea and dimethyl ether. A particular type of chemical conversion used is the methanation process, whereby CO₂ is converted into the more desirable product of methane. The methanation process involves two major steps: the partial reduction of CO₂ to CO as an intermediate state, followed by the hydrogenation of the CO³. The conversion of CO₂ to CH₄ is significant is due its potential for both the chemical capturing of CO₂ and the storage of hydrogen in the form of a condensable gas. This can be utilised in a range of applications including: commercial power stations for the generation of electricity⁴ and the refining of petrochemicals⁴. It is also the major component found in natural gas, typically used for heating and cooking⁴. A major limitation of the current methanation reaction is the low yield of products making the capture of CO₂ uneconomical⁴. This is primarily due to the consumption of high levels of energy via high temperatures and pressures needed⁴. The general chemical equation for the conversion of CO₂ to CH₄ is: $CO_2 + 4H_2 \rightarrow CH_4 + 2H_2O$.

The simplicity of the reaction masks inherent challenges in that in order for the reaction to progress to completion, reaction and catalyst conditions need to be considered⁴. With conventional methanation processes, metal-based catalysts (including nickel, palladium and platinum-based) are typically utilised in addition to maintaining reaction temperatures at approximately 600- 800 °C. In addition to costs covering the relatively high energy consumed by these reactions, extra costs will need to be considered for the purchase of reaction vessels capable of withstanding high temperatures and pressures⁴.

Another limitation of using conventional catalysts is the formation of coke as a byproduct. Coke has been shown to act as a good deactivator of catalysts in reactions where there is limited oxygen available. Previous research has shown the direct correlation between the deposition rate of coke and temperature⁴. Thus as the temperature of the reaction increases, the deposition rate of coke similarly increases⁴. However, alternative methanation reactions currently being proposed by researchers eliminate such problematic issues by implementing the use of organo-boron based catalysts, which would ideally eliminate the amount of CO byproduct being produced in the final product and operate at or near ambient conditions.

With the understanding of such limiting factors and continuing advancement in technology, researchers have investigated both metal and metal-free catalysts. Consequently, research in the area of catalysis has rapidly increased with a demand for cheaper catalyst designs to provide high yield products, as well as an outlook into the regeneration of catalysts in situ.

This introduction will primarily outline the conversion of CO₂ into hydrocarbons, with a specific outlook into the production of methane, a simple hydrocarbon compound. The review will also focus on the state of the art regarding conventional approaches being utilised when determining types of catalysts used, the methodologies implemented and the associated reaction mechanisms being proposed. Additionally, alternative approaches to methanation utilising organo-boron based catalysts will be discussed, where the project aims and methodologies are proposed.

1.2 Conventional approaches to CO₂ to CH₄ conversion

Conventional approaches to CO₂ reduction normally involve the direct reduction of CO₂ using diatomic hydrogen over a catalyst which is typically metal based.

The term ‘catalysis’ was first introduced by Berzelius in 1836 for providing explanations towards reactions which undergo transformations and decompositions⁵. A catalyst is most commonly defined as a reagent providing an alternative route for the reaction to progress⁶. Such alternate pathway involves the catalyst interacting (which involves forming bonds) with the reactants, creating an activation pathway with a lower activation energy and a greater reaction rate as illustrated in figure 1⁶. Theoretically, an ideal catalyst remains unchanged throughout a reaction; however, this is typically not the case when put into practice. Often, the catalyst chemically bonds with the reactants used, which over time leads to deactivation⁵. Therefore, there is currently an increased demand in the regeneration or recycling of catalysts. When wanting to implement or validate the use of a particular catalyst within a reaction

system, a variety of analytical and microscopic techniques may be applied for their characterisation. Such methods include: GC-MS, NMR, XRD, TEM and FTIR ⁷.

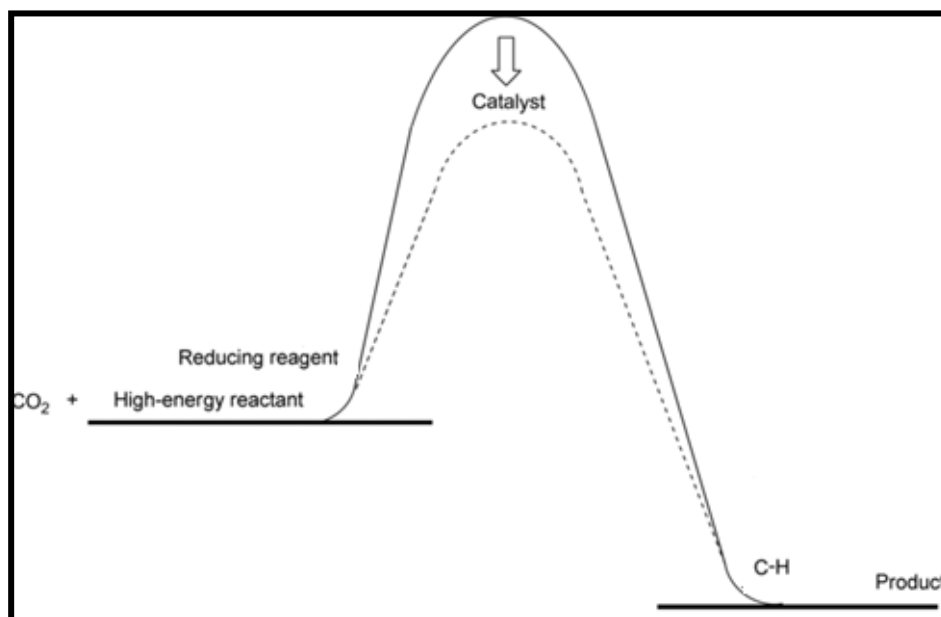


Figure 1. The process involved for the conversion of CO_2 . As a minimal requirement, CO_2 and a high energy reducing reagent are required in addition to a catalyst, which will provide an alternative pathway for the reaction to progress to completion using a smaller activation energy, in order of reducing the $\text{C}=\text{O}$ bond to a C-H bond ⁸.

Without considering the time, efforts and costs involved in the capturing and separation of CO_2 from its sources (generation power plants and other sources where the combustion of fossil fuels occur), the actual process involving the conversion of CO_2 to hydrocarbons is not a simple feat. The CO_2 molecule is extremely stable, requiring specific types of catalysts to break the bonds between the atoms involved. Ultimately for methane to be synthesised, CO_2 needs to be reduced which requires sufficient energy in order to break the strong $\text{C}=\text{O}$ bonds of the molecule. Attempts have been made to overcome this energy barrier through the use of solar activated photocatalytic splitting of water and reduction of CO_2 ⁹. Photocatalytic catalysis is highly desirable as it provides an environmentally sustainable method of reducing atmospheric CO_2 .

Compared to the use of heterogeneous catalysis, homogeneous catalysis can also be utilised where both reactants and catalyst interact and react within the same phase. The advantage of using this method is that widely dispersed reactants and catalysts allow for ease of access by dissolved CO_2 to the active site(s) present ⁹. However, the major limitation associated with using homogeneous catalysts involves use of expensive metal-based catalysts. These reactions also require reducing agents that are completely consumed as part of the reactions, thus requiring continuous supply ⁹. As a result, there has been an increasing demand for the development of novel catalysts with specific physicochemical properties which can

ultimately reduce the costs involved as well as the reduction of chemical conditions being applied (temperature and pressure).

Radical thoughts currently in use for regeneration of organo-boron based catalysts include incorporation of silica aerogels¹⁰ as a solid platform. At this point, the boron-based catalyst will adsorb it, resulting in a boron-silicon based solid phase complex by which the catalyst and reducing reagents can potentially be regenerated in situ. Particular physicochemical properties associated with these silica-based aerogels include: approximately 95 % based composition made up of air (giving an overall low bulk density), large surface area and relatively low thermal conductivity¹⁰.

Regarding the conversion of CO₂ to CH₄, the CO₂ molecule must be first activated. For this reason, both thermodynamic and kinetic aspects behind the conversion process need to be considered to decide which catalysts, reagents, experimental parameters and conditions need to be utilised. Activation of CO₂ is relatively difficult due to its thermodynamic stability (arising from its Gibbs free energy) in addition to its inert properties⁸. In terms of structural composition, the CO₂ molecule is linear and non-polar with two reactive carbonyl sites, in which the carbonyl carbon is electron deficient. Thus, CO₂ has a strong affinity towards reducing agents⁸, which silanes have been shown to act as particularly good reducing agents¹¹. In summary, the minimal reagents required for the production of C-H bonds in the CH₄ product include: CO₂, a high energy reducing reagent and a catalyst. This reaction system will be subjected to relatively high pressures and varying temperatures, to determine optimal experimental parameters and conditions required for greatest reaction rates and efficiencies shown, quantitative determination via real-time MS % yields.

1.3 Problems faced regarding conventional approaches

One of the major issues facing the use of heterogeneous hydrogenation of CO₂ are the reaction usually needs to be carried out under high temperatures typically exceeding 600 °C⁴.⁹ Research has also shown the implementation of metal-based catalysts result in relatively low levels of selectivity and activity, requiring high levels of energy⁹. By incorporating metal-based catalysts, methanation reactions are often left incomplete, forming products including carbon monoxide and unreacted carbon dioxide⁹. The reaction system and experimental design put forward within this project will ultimately address the current problems already suggested, providing further insight into regeneration of catalysts and reducing reagents in situ.

Additionally, obtaining hydrogen sources for methanation reaction are another major problem. These processes involve the burning of fossil fuels and degradation of biomass.

Method limitations include requirements of high temperatures and pressures and availability of steam and oxygen⁹. Future research directions may involve implementing ‘cleaner’ alternatives including renewable hydroelectric resources such as wind, solar and geothermal energy⁹.

1.4 Alternate approaches to the conversion of CO₂ to CH₄

Radical thoughts currently researched for the conversion of CO₂ involves the heterolytic cleavage of H₂ by amines and B(C₆F₅)₃, breaking the intramolecular H₂ bond, forming ion pairs which synthesises the tandem catalyst.

As shown in Figure 2, the thermal dissociation of the B-N bond between the Lewis-acid and Lewis-base occurs via cleavage of the strong dihydrogen bonding present, resulting in a Lewis-acid Lewis-base adduct¹². This Lewis-acid Lewis-base adduct is termed a frustrated Lewis pair (FLPs); defined as the combination of a sterically strained Lewis-acid and Lewis-base involved in a strong donor-acceptor interaction framework¹³. The FLPs are presented as a separate group in comparison to what would be defined as a “normal” Lewis pair, which is the neutralised product of a classical Lewis acid/ Lewis base adduct¹⁴.

Related research includes a study focused on utilising B(C₆F₅)₃ and n-butylsilane as a reducing reagent without the presence bulky amines for conversion of polycarboxylic acids into its corresponding alkanes¹⁵. Based on this study and others alike, the use of a bulky amine was deemed unnecessary. However, bulky amines are required for the heterolytic cleavage of H₂ for synthesis of the tandem catalyst. This project will also consider whether the incorporation of bulky amines is required to obtain optimum yields of CH₄.

Additionally, using a good reducing agent involves incorporating an effective catalyst. In 1995, tris(pentafluorophenyl)borane was proposed, ultimately allowing for the formation of Frustrated Lewis Pairs (FLPs)¹⁶. Properties of the catalyst include: air stability, thermal stability (up to 270 °C), very stable B-C bonds and electronegative fluorine groups; ideal for the reaction with silane-based Lewis-acids¹⁶. This project will incorporate the B(C₆F₅)₃ alone and also by synthesising the tandem catalyst using a bulky amine to determine whether there is any effect on the activity, selectivity, efficiency and rate of reaction for the conversion of CO₂ to CH₄.

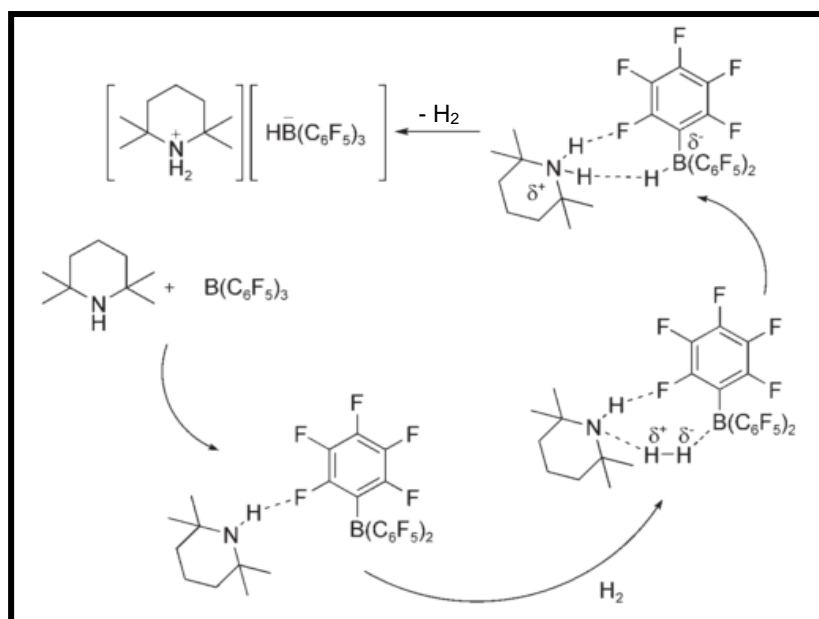


Figure 2. Heterolytic cleavage of H₂ by amines and B(C₆F₅)₃. The thermal dissociation of the B-N bond, resulting in a Lewis-acid Lewis-base adduct ¹².

The synthesis of the tandem catalyst is particularly significant as it is incorporated into the reaction involving the activation of CO₂ and a silane reducing agent under relatively mild temperatures and pressures ¹³. The products formed include methane along with a siloxane byproduct in a 1:2 ratio, as shown in Figure 3. Therefore, regeneration of the silane reducing reagent from the siloxane byproduct would be ideal, breaking the conventional notions using relatively expensive sacrificial metal-based catalysts.

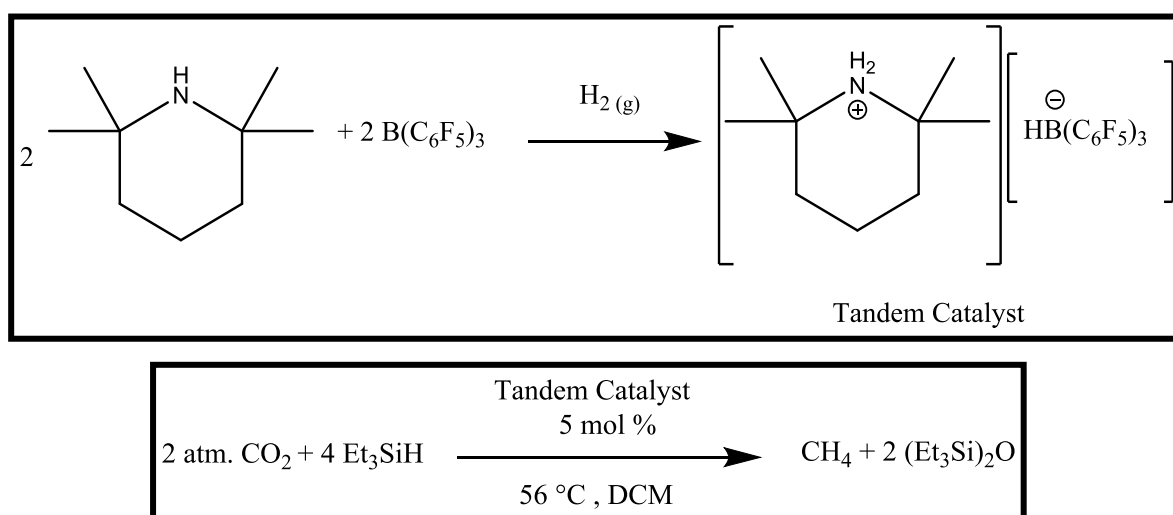


Figure 3. Activation of CO₂ by the FLP under relatively mild conditions redrawn from ¹³.

Siloxanes are a subgroup of the silicone family known for their “Si-O-Si” linkage and are widely characterised by their non-toxic and volatile behaviours. When combusted they form crystalline silica products which are known to stick onto surfaces of commercial instruments, causing significant buildup of heat ¹⁷. As a result, operators are required to continuously replace equipment parts including turbochargers and engines costing companies a significant amount of time and money ¹⁷. Therefore, companies are now engineering instruments which will ultimately separate siloxanes produced using methods such as non-regenerative adsorption materials ¹⁸. However, these processes are only applied to siloxane byproducts formed from non-methanation processes. These methods do not solve the issue of siloxanes being produced but rather contribute even further to their accumulation within various environments including the atmosphere and landfills ¹⁸. This also means that companies have to spend even more time and money purchasing and installing the systems used for separation. An alternative solution to this issue would be to regenerate the silane reducing agents from siloxane byproducts which can then be recycled within the methanation process.

Siloxanes are typically characterised using techniques including GC-MS and FTIR. The bending modes of siloxanes are commonly found at wavenumbers between 475-500 cm⁻¹, whilst their stretching modes are commonly found at 1000-1130 cm⁻¹ ¹⁹.

1.5 Considerations for the silane reducing reagents being used

Considerations must also be made regarding types of silanes used within the project. Reasons for this include thoughts related to the silicon-containing byproducts formed once the methanation reaction has gone to completion. The byproducts typically formed when using tri-substituted silanes include silanols; whereas using mono- or di-substituted silanes typically result in silicone byproducts ¹¹.

Research conducted by Nimaggada and McRae (2006) showed reduction of carboxylic acids, ketones, alcohols, aldehydes and methyl esters to alkanes using B(C₆F₅)₃ and either n-butylsilane or diethylsilane as reducing reagents ^{15, 20}. These reactions are particularly beneficial due to their convenient and time-efficient one-pot reaction system. They also provide a means for reducing only polar functional groups found on the compounds ²⁰.

Previous research conducted had shown the B(C₆F₅)₃ catalyst is sensitive to steric resistance around the Si-H bond. An example is triethylsilane, which presented a lower rate of reaction in comparison to dimethylethylsilane ¹¹. Another result discussed bulkier silanes reacting through a similar mechanism, however requiring greater amounts of catalysts to be used in addition to longer reaction times for achieving the final product ¹¹. In a similar manner, if the silanes in use were not structurally bulky the reaction would not progress to

completion unless temperatures and pressures are increased. Si-H bonds have a relative Gibbs free energy of approximately 380 kJ mol^{-1} which is 20 % less than the H-H bond found in H_2 ¹¹. These results bring forward the need to further investigate effects of various boron-based catalysts in conjunction with a range of silanes, measured using various experimental conditions (such as temperatures and pressures).

From this research and similar research, the reaction system being proposed could similarly be manipulated to directly target the reduction of the siloxane byproducts back into silane reducing reagents. Ideally catalyst(s) used could also be regenerated in situ, resulting in a continuous closed system for the conversion of CO_2 to CH_4 .

1.6 Proposed Project

This project will be focused around three major aims:

1. Developing an experimental setup for small scale methanation reactions.
2. Screening a variety of silane-based reducing agents against three different forms of catalysts; $\text{B}(\text{C}_6\text{F}_5)_3$, the synthesised tandem catalyst and $\text{B}(\text{C}_6\text{F}_5)_3$ +tandem catalyst to determine the efficiencies (via relative GC-TCD % yield) and rates of reaction (via relative MS % yield) for the formation of CH_4 within the methanation process.
3. Determining the effect of bulky amines on the formation of the Lewis acid/Lewis base adduct (the tandem catalyst) and their contribution to the methanation process.

Furthermore, techniques for the continuous regeneration of siloxane byproducts into silane reducing reagents will be investigated. These investigations would further justify the aims of the project as the whole system would be closed (and carbon neutral) where all reagents are ultimately regenerated in situ. This project is significant as no research has been previously conducted for the screening of a range of silanes against various catalysts, in particular screenings involving the tandem catalyst. This project has the potential for further investigations including implementing the catalytic system into a silicon-based (reducing) solid framework; allowing the reaction to take place within a solid phase. This idea would take advantage of the $[\text{B}]^{\delta-} \cdots \text{H} \cdots [\text{Si}]^{\delta+}$ interaction present during the heterolytic cleavage of H_2 for the formation of the tandem catalyst. Applications relevant to this framework include the capturing and storage of hydrogen and methane.

The significance of this project involves the use of a boron-based catalyst and silane reducing agent, which acts as a good framework for capturing CO_2 and forming CH_4 and can be easily stored. With the screening of a range of silanes against three forms of catalysts, the optimum reagents can be determined, resulting in faster reaction rates for the conversion of CO_2 to CH_4 in addition to higher yields of CH_4 formed. The improvement of these two major

parameters using milder experimental conditions compared to those already researched and reported will ultimately consume less energy, making the whole process economically desirable.

1.7 Summary of Methodologies

In summary, the major aim of the project is to determine the efficiencies and rates of reaction for the methanation process by screening a variety of silane-based reducing agents against three forms of boron-based catalysts. The efficiencies will be determined via real-time MS and GC-TCD measurements, whereby reaction rates for the formation of CH₄ will be compared.

These project aims can ultimately be achieved by using the following methodologies:

- The design and manufacture of an experimental setup where the methanation process can take place. The setup will consist of custom designed reaction vessels within a gas retaining cylinder used for the containment and reaction of blended experimental gases.
- The synthesis and characterisation of the tandem catalyst using a compound with a bulky amine functional group. Characterisation of the tandem catalyst will be performed using FTIR, NMR and GC-MS.
- The monitoring and quantitative analysis of the forward reaction for the conversion of CO₂ to CH₄ using a real-time MS system, determining the rates of reactions. Quantitative data will also be reported using the GC-TCD to determine relative yields of CH₄ formed.
- Methanation will be performed using the following catalysts: synthesised tandem catalyst alone, B(C₆F₅)₃ alone and combination of tandem catalyst and B(C₆F₅)₃.
- The methanation will also be performed using the following reducing reagents: diethylsilane, triethylsilane, n-butylsilane and hexylsilane.
- The characterisation of the siloxane byproducts using FTIR.
- The reduction of the siloxane byproducts back into the silane reducing reagents using: (i) H-cube® continuous-flow hydrogenation reactor, (ii) the photoreduction of siloxanes using short wavelength UV light supplied via high powered low pressure Mercury Vapour Lamp (iii) the electrochemical reduction of siloxanes using cyclic voltammetry.
- The characterisation of the regenerated silane reducing reagents using GC-MS and/or FTIR.

Chapter 2: Experimental

2.1 Materials

The following chemicals were purchased and used without additional purification: $\text{B}(\text{C}_6\text{F}_5)_3$ (Sigma-Aldrich, 95 %), toluene (Sigma-Aldrich, 99.8 % anhydrous), chloroform (Sigma-Aldrich, ≥ 99.5 %), 2,2,6,6-tetramethylpiperidine (Sigma-Aldrich, ≥ 99 %), diethylsilane (Sigma-Aldrich, 99 %), triethylsilane (Sigma-Aldrich, 97 %), n-butylsilane (Sigma-Aldrich, ≥ 97.0 %), hexylsilane (Sigma-Aldrich, ≥ 97.0 %), chloroform-d (Sigma-Aldrich, 99.8 atom % D), chlorotrimethylsilane (Sigma-Aldrich, ≥ 97 %), ethanol (undenatured, 100 %), heptanoic acid (Sigma-Aldrich, 96 %), dichloromethane (anhydrous, Sigma-Aldrich, ≥ 99.8 %), decane (Fluka, analytical standard), dodecane (Sigma-Aldrich, ReagentPlus, ≥ 99 %), oxalic acid (Sigma-Aldrich, ReagentPlus, ≥ 99 %) and cyclohexane (Sigma-Aldrich, ≥ 99.9 %).

Drying agents were added to any anhydrous containing solvent bottles (toluene and chloroform) to ensure all residual water molecules are captured and not introduced into any reactions. Activated 3 Å molecular sieves (10 hours at 450 °C) were used to dry the chloroform and sodium wire was used for the toluene.

All vessels containing moisture sensitive reagents and solvents were purged with dry Argon gas prior to and after use. These include: diethylsilane, triethylsilane, n-butylsilane, hexylsilane, chloroform and toluene.

The gases used were supplied by BOC Australia and were of high purity grade or better.

2.2 Equipment and Instrumentation

Any handling of moisture sensitive solid compounds was carried out in an Argon filled glove bag (Sigma-Aldrich, AtmosBag, Size M, Product #Z530212). All pipetting was performed using an eVol XR autopipette (SGE Analytical Science, product #2910205).

2.2.1 Real-time MS

Real-time MS analysis was carried out on the Balzers quadrupole mass spectrometer QMS 422 (ThermoStar Instruments) gas analyser. The program used to process and collect data was QUADSTAR 422 (Version 7.0). The inlet of the mass spectrometer consisted of a heated quartz capillary (SGE Analytical Science 0.32 mm ID Deactivated Fused Silica Capillary Tubing (2.76 m)) for analysing samples at the pressure of 15 psig. An additional length (11 cm) of 0.22 mm ID Deactivated Fused Silica Capillary Tubing was connected to

the heated inlet to act as a restrictor to allow direct interface to the pressure reaction vessel and still maintain optimal operating vacuum in the MS, when analysing samples at a pressure of 15 psig. The appropriate pressure level was at approximately 10^{-5} mbar which was optimal for the MS. The heated interface line was operated at 120 °C and left on at all times prior to and during experimentation. Operating conditions used as part of the real-time MS method are detailed in the table below.

Table 1. Operating conditions of MS used for two method files.

Method File Name		
<i>sr 29 psig 3 atm.mcp</i>		
<i>sr 15 psig 2 atm.mcp</i>		
Details	Value	Units
<i>Measurement Parameters- Detector</i>		
State		
Channel-0	MATRIX	-
Channel-1	MATRIX	-
Channel-2	MATRIX	-
Channel-3	MATRIX	-
Channel-4	ENABLE	-
Mass		
Channel-0	14	amu
Channel-1	15	amu
Channel-2	40	amu
Channel-3	44	amu
Channel-4	-	-
SEM Voltage		
Channel-0	1400	V
Channel-1	1800	V
Channel-2	1400	V
Channel-3	1400	V
Channel-4	-	-
<i>Measurement Parameters- Mass</i>		
Dwell		
Channel-0	0.5	s
Channel-1	0.5	s
Channel-2	0.5	s
Channel-3	0.5	s
Channel-4	-	-
Resolution		
Channel-0	10	-
Channel-1	12	-
Channel-2	35	-
Channel-3	40	-
Channel-4	-	-
<i>Measurement Parameters- Amplifier</i>		
<i>Ion Source Parameters- Ion Source</i>		
Type	HS Yttria	-
Filament #	Fil 2	-

Set #	SET 0	-
<i>Ion Source Parameters- IS Emission</i>		
Emission Current	1.00	mA
Emission Protect	3.50	A
<i>Ion Source Parameters- IS Voltages</i>		
Ion Ref	105	V
Cathode	70.00	V
Focus	4.00	V
Field Axis	14.00	V
Extraction	17	V
RF-Polarity	inverse	-
<i>State Parameters</i>		
Normalization Mode	SUM = 100	%
Negative Concentration Suppression	ON	-
Mass Scale Correction	ON	-
Zero Gas Subtraction	ON	-

When using the MS to monitor the formation of methane, the Multiple Concentration Detection (MCD) mode was utilised. Prior to running the samples using MCD mode, calibration gas standards of the same relative mol % were used at the two pressures being measured, at which point the “gas calibration” was selected on the Measurement program of the INFICON QUADSTAR software (32 bit). Based on the relative concentrations of each of the gases using within the calibration standards and the level of current detection of each gaseous ion, the instrument takes these calibration factors into account when reporting the actual data points during sample runs. As a point of reference, the calibration factors used at the two pressures analysed are reported in the table below.

Table 2. The MCD matrix set up taken from the gas calibration values obtained during standard runs. Note that no direct relationship can be established between the calibration factors used to analyse samples at 15 and 29 psig, as different interface lines were used for each calibration.

Method File Name		<i>sr 15 psig 2 atm.mcp</i>	<i>sr 29 psig 3 atm.mcp</i>
Mass / amu	Gas Component	Value	Value
<i>MCD Matrix Parameters</i>			
14.13	N ₂	4.170	56.61
15.16	CH ₄	74.29	11.08
40.00	Ar	1.000	1.000
44.00	CO ₂	0.8272	2.125

2.2.2 GC-MS

GC-MS analyses were carried out on a Shimadzu GC-17A (Ver. 3) Gas Chromatography coupled with a Shimadzu QP5000 Quadrupole MS detector. GC-MS data was collected and

analysed using Shimadzu GCMS Solution (Version 2.40). Separations were performed on a Restek Rtx-5Sil MS capillary column (Product #12723, Crosslinked, 95 % dimethyl polysiloxane, 5 % diphenyl polysiloxane, 30 m, 0.25 mm ID and 0.25 μm). The operating conditions used as part of the GC-MS method are details in the table below.

Table 3. Instrumental conditions for GC-MS used for two separate method files.

Method File Name	<i>sil_syn.met</i>	<i>sil_silo.met</i>	
Details	Value	Value	Units
Carrier Gas	Helium	Helium	-
Sample Volume	0.1	0.1	μL
<i>Gas Chromatograph Program</i>			
Oven Temperature	40.0	40.0	$^{\circ}\text{C}$
Oven Equilibrium Time	1.00	1.00	min
Injector Temperature	270.0	270.0	$^{\circ}\text{C}$
Interface Temperature	300.0	300.0	$^{\circ}\text{C}$
Injector Mode	Split	Split	-
Column Flow	1.5	1.1	mL/min
Linear Velocity	44.2	38.7	cm/s
Injector Split Ratio	190	200	-
<i>Mass Spectrometer Program</i>			
Start m/z	40.00	40.00	-
End m/z	600.00	600.00	-
Scan Interval	0.20	0.20	s
Threshold	3000	3000	-
Scan Speed	4000	4000	amu/s
<i>Acquisition Time</i>			
Program Time	28.00	28.00	min
<i>Realtime Monitor</i>			
Detector Volts	1.20	1.20	kV

The instrumental conditions described under the method file name “sil_syn.met” were used for: characterisation of $\text{B}(\text{C}_6\text{F}_5)_3$, synthesis of the tandem catalyst and synthesis and H-cube reductions of ethoxytriethylsilanes. The conditions described under the file name “sil_silo.met” were used for: methanation sample reactions, syntheses, photoreduction analyses and electrochemical reductions of hexaethyldisiloxanes. Compound identifications were performed using the NIST21, NIST107 and Wiley9 libraries.

2.2.3 GC-TCD

GC-TCD analyses were performed on a Shimadzu GC-14B Gas Chromatograph fitted with a Thermal Conductivity Detector. GC-TCD data acquisition was performed and processed using the Shimadzu GC Solution (2.21.00 SU1). Separations were performed on an Agilent J&W GS-CARBONPLOT GC Column (Product #113-3133, bonded monolithic carbon layer stationary phase, 30 m, 0.32 mm ID and 3.00 μm). The operating conditions used as part of the method are detailed in the table below.

Table 4. Operating conditions of the GC-TCD method file used.

Method File Name <i>split.met</i>		
Details	Value	Units
<i>TCD Program</i>		
Sampling Frequency	5	Hz
Run Time	8	min
<i>Instrumental Conditions</i>		
Mode	Split	-
Carrier Gas	Helium	-
Carrier Gas Pressure	170	kPa
Carrier Flow	30	cm/s
Column Temperature	35	$^{\circ}\text{C}$
Injection Temperature	110	$^{\circ}\text{C}$
Detector Temperature	120	$^{\circ}\text{C}$
TCD Temperature	120	$^{\circ}\text{C}$
TCD Current	100	mA
Polarity	INJ1(+)	-
Split	1:13	-

As shown within the table above, the conditions for the GC-TCD instrument under the method file named “split.met” was used for the analysis of each sample. GC-TCD was used to analyse the static head-space of the methanation reactions. When GC-TCD was being used the 3-port valve (see Figure 10) was closed preventing passage of the reaction mix into the MS. At a fixed time point (10 minutes) for all the reactions the 3 port valve was turned to open the line connecting the reaction vessels to a previously connected gas tight syringe (SGE Analytical Science, 2.5 mL, product #008687, screw thread). A volume of 1 mL of the

reaction head space was collected. The Luer Lock fitting was removed from the tip of the syringe and replaced using a NM1/2.5(EVOL 500UL)-5/0.63D needle (SGE Analytical Science, dome shaped, product #039116) and the gas sample injected into the GC-TCD.

The sample matrix and sample identifiers used for the methanation process, real-time MS analysis and GC-TCD analysis are detailed in tables below.

Table 5. The experimental sample matrix for 15.00 psig.

Catalyst	Silanes @ Pressure= 2 atm. ~ 15.00 psig Direct Measurement MS			
	diethylsilane	triethylsilane	n-butylsilane	hexylsilane
No Catalyst(s)	S017	S018	S019	S020
TC	S001	S002	S003	S004
$B(C_6F_5)_3$	S013	S014	S015	S016
$B(C_6F_5)_3 + TC$	S009	S010	S011	S012

Table 6. The experimental sample matrix for 29.00 psig.

Catalyst	Silanes @ Pressure= 3 atm. ~ 29.00 psig Direct Measurement MS			
	diethylsilane	triethylsilane	n-butylsilane	hexylsilane
No Catalyst(s)	Si05	Si06	Si07	Si08
TC	S021	S022	S023	S024
$B(C_6F_5)_3$	S025	S026	S027	S028

Specific tables providing more information regarding each of the samples and what volumes of silane stock solutions were added to each are detailed within Appendix 6.

2.2.4 FTIR

FTIR spectra were obtained using the Thermo Scientific Nicolet iS10 FT-IR Spectrometer, using either the Smart iATR accessory or the Smart Collector accessory. Specifically, the Smart iATR accessory was used for collecting Attenuated Total Reflectance (ATR) spectroscopic data and the latter used for collecting Diffuse Reflectance Infrared Fourier Transform (DRIFT) spectroscopic data. All IR data were collected and processed with OMNIC (Thermo Scientific, Version 8.2.388). Background scans for DRIFT were performed before every sample analysed using spectroscopic grade KBr powder which was ground using a mortar and pestle. The instrumental parameters and conditions for the spectroscopic modes used are outlined within Table 7.

Table 7. Instrumental conditions and parameters used for ATR and DRIFT spectroscopic modes.

Parameters	Attenuated Total Reflectance Spectroscopy (ATR)	Diffuse Reflectance Infrared Fourier Transform Spectroscopy (DRIFT)	Units
IR Range	4000-650	4000-400	cm ⁻¹
Resolution	4.000	4.000	cm ⁻¹
Number of Scans	16	150	scans
Apodization	Boxcar	Boxcar	-
Correction	Automatic Baseline	Automatic Baseline	-
Aperture	80.00	80.00	-
Optical Velocity	0.4747	0.4747	-
Sample Gain	8.0	8.0	-
Mode	Absorbance	log(1/R)	-
Window	Diamond	Diamond	-
Detector	DGTS KBr	DGTS KBr	-

2.2.5 NMR

All ¹H and ¹³C NMR experiments were performed on a Bruker Avance DPX 400 MHz spectrometer equipped with a TXI (5 mm) Cryoprobe. Chemical shifts were reported in ppm using residual CHCl₃ as an internal reference (δ H; 7.26 ppm, δ C; 77.5 ppm²¹). The pulse lengths used for the high power ¹H p/2 was ~9.5 ms, and for the high power ¹³C p/2 was 11.05 ms. All spectral data were processed using Bruker Topspin (version 1.3).

2.2.6 Data Processing

All quantitative data acquired from individual instrumentation programs and software were analysed and processed using Microsoft Excel (2010).

2.3 Synthetic Procedures and Characterisation

2.3.1 B(C₆F₅)₃ characterisation

The catalyst tris(pentafluorophenyl)borane was characterised using NMR. A small amount of B(C₆F₅)₃ (19.3 mg, 0.0000377 mol) was dissolved in deuterated chloroform

(CDCl₃) and introduced into a clean NMR tube. This was performed within the argon filled glove bag. ¹³C NMR (400 MHz, CDCl₃) δ 216.26, 201.51, 173.49 ppm.

For GC-MS analysis, B(C₆F₅)₃ (10.7 mg, 0.0000209 mol) was placed into a clean, oven dried sample vial and dissolved in CHCl₃ (1 mL). The sample vial was inverted a couple of times before being directly injected into the GC-MS. (MS (DI, EI) [m/z (%)]: 83.15 (100), 85.10 (67.52), 47.00 (40.44), 48.10 (16.20), 49.05 (12.53), 86.90 (12.40), 50.10 (5.04), 118.05 (2.31), 120.00 (1.88), 117.00 (1.69), 41.35 (1.51), 119.05 (1.51), 69.90 (1.10), 71.90 (0.75), 121.95 (0.67), 42.50 (0.62), 121.05 (0.45), 88.00 (0.16), 58.50 (0.12), 59.50 (0.12).

For FTIR (ATR) analysis, a small amount of the solid catalyst was placed onto the sample platform of the ATR FTIR instrument. Prior to analysis, the FTIR instrument was purged with N₂ gas until signal was stabilised for the background reading. The background reading was taken of the clean platform surface prior loading the catalyst sample. (IR (ATR): 3685.36, 3590.49, 1649.61, 1521.17, 1459.67, 1378.16, 1282.46, 1103.62, 1090.04, 968.31, 868.23, 772.74, 667.84 cm⁻¹).

2.3.2 Synthesis of the tandem catalyst ¹²

Tris(pentafluorophenyl)borane (848 mg, 0.00129 mol) was placed into a clean teflon sealed vial (10 mL) containing a magnetic stirrer in an argon filled glove bag. The pressure vial was then sealed and purged with argon gas under the fumehood. To this, dry toluene (5 mL) was added to the pressure vial using a gas tight syringe. 2,2,6,6-tetramethylpiperidine (0.220 mL, 0.00129 mol) was added to the pressure vial using another clean gas tight syringe. The reaction mixture was allowed to mix on the magnetic stirrer in order of obtaining a homogenous solution and was purged with argon gas. Using a 22 Gauge (1.5", Luer lock) needle connected to a PP/PE needle (10 mL), a balloon filled with hydrogen gas (1 atm) was connected to the end of the needle using Parafilm. The needle was inserted into the Teflon lined pressure vial, and the reaction mixture was allowed to stir (750 rpm) at room temperature for 1 hour. All volatiles were removed using a vacuum oven set at 60 °C. Once dry, the reaction resulted in a white-coloured product (656 mg, 0.00100 mol, 77.4 %, ¹H NMR (400 MHz, CDCl₃) δ 1.310 (12H, s), 1.592-1.620 (4H, t), 1.739-1.749 (2H, d), 6.919 (2H, s), ¹³C NMR (400 MHz, CDCl₃) δ 149.210, 147.328, 138.005, 135.986, 58.115, 35.844, 27.650, 16.076, MS (tandem catalyst in CHCl₃) (DI, EI) [m/z, (%)]: 83.15 (100), 85.15 (68.38), 47.00 (41.75), 48.10 (16.88), 49.05 (13.05), 86.90 (12.64), 50.05 (5.34), 118.00 (2.31), 119.95 (1.93), 117.00 (1.68), 41.30 (1.56), 119.00 (1.55), 69.90 (1.14), 71.85 (0.76), 42.45 (0.66), 121.95 (0.65), 121.00 (0.47), 88.05 (0.15), 58.50 (0.14), 73.90 (0.12), IR (ATR):

3662.02, 3269.59, 1643.87, 1514.72, 1456.23, 1388.58, 1267.50, 1080.53, 962.01, 945.41, 770.99, 763.77, 736.85, 726.89, 670.45 cm⁻¹).

2.3.3 Synthesis of Siloxane reagents

2.3.3.1 Synthesis of ethoxytrimethylsilane mixture ²²

The mixture containing various forms of ethoxytrimethylsilanes was prepared by reacting ethanol (2 mL, 0.034 mol) with chlorotrimethylsilane (6.70 mL, 0.053 mol) for 25 minutes at 100 °C. The product obtained was a light yellow coloured liquid.

Using GC-MS analysis, the various siloxane components of the mixture were identified as; ethoxytrimethylsilane, hexamethyldisiloxane, unreacted triethylsilane, diethoxydimethylsilane, ethylpentamethyldisiloxane, 1,3-diethyl-1,1,3,3-tetramethyldisiloxane, octamethyltrisiloxane, 1,3-diethoxy-1,1,3,3-tetramethyldisiloxane, hexamethylcyclotrisiloxane, decamethyltetrasiloxane and 3-ethoxy-1,1,1,5,5,5-hexamethyl-3-(trimethylsiloxy)trisiloxane. 0.1 µL of the neat product was injected into the MS source. (MS (DI, EI) [m/z, (%)]: 103.10 (100.00), 75.05 (98.24), 58.95 (45.13), 73.00 (41.55), 45.05 (41.44), 43.05 (21.55), 47.05 (13.83), 61.05 (10.72), 104.20 (9.56), 44.10 (9.02), 76.15 (6.34), 51.00 (5.53), 105.15 (4.42), 42.05 (3.93), 60.10 (3.65), 58.05 (3.47), 77.05 (3.02), 46.15 (2.80), 54.90 (2.06), 57.10 (1.51)).

2.3.3.2 Synthesis of hexaethyldisiloxane ¹⁵

An oven dried vial (mL) was purged with argon. Heptanoic acid (141.8 µL, 0.001 mol) was measured into the vial and argon purge resumed. B(C₆F₅)₃ (24.0 mg, 5 mol %) was then added as part of a solution prepared containing anhydrous dichloromethane (5 mL). The solution was allowed to stir for 10 minutes before adding triethylsilane (638.9 µL, 0.004000 mol). A static atmosphere was maintained using an argon balloon (1 atm). The reaction mixture was stirred for 20 hours at room temperature. Reaction progress was monitored by GC-MS until the product was observed; obtaining a transparent solution. To this product, decane (637 µL, 1 mass equivalence ratio to silane used) was added to the pressure vial. The decane acts as an internal standard for the photochemical reduction experimentation.

The same reaction detailed above was performed using oxalic acid to produce various lengths of siloxane products. The oxalic acid (0.09003 g, 0.001000 mol) was reacted with B(C₆F₅)₃ (25.6 mg, 5 mol %) and produced a transparent product. (MS (DI, EI) [m/z, (%)]: 161.15 (75.62), 65.95 (62.76), 59.00 (40.41), 80.10 (36.37), 105.00 (34.44), 133.10 (25.28), 103.00 (15.92), 94.05 (15.17), 52.10 (15.03), 76.95 (12.03), 87.00 (10.24), 56.95 (9.28),

131.10 (8.67), 73.00 (7.34), 159.15 (6.90), 67.05 (5.76), 45.05 (5.46), 75.00 (4.74), 88.80 (4.22), 90.95 (3.89)).

2.3.4 Nickel Zeolite Catalysts^{5,23}

3 Å (Sigma Aldrich, beads, 4-8 mesh, product #208574), 4 Å (Sigma Aldrich, beads, 8-12 mesh, product# 208590) and 5 Å (Sigma Aldrich, beads, 30-40 mesh, product# 20300) molecular sieves (3 g) were newly taken out of the bottles and put into three separate clean ceramic crucibles. 20 mL of a 0.2 mol L⁻¹ nickel acetate solution was added to each crucible which was then swirled to ensure the zeolite surfaces were coated in the nickel acetate solution. This allowed the nickel to be introduced to the zeolites via adsorption (incipient wetness).

The crucibles were placed into the furnace oven and calcinated in dry air at 500 °C for 8 hours. Once removed, the samples were allowed to cool under N₂, and stored within sample vials (20 mL capacity) and sealed using Parafilm. The calcinated zeolites were analysed using DRIFT FTIR. (IR (DRIFT): (3 Å) 3443.27, 1659.78, 1119.78, 684.80, 675.61, 539.04, 483.18, 406.21 cm⁻¹, (4 Å) 3459.48, 1649.67, 999.66, 459.65, 471.19 cm⁻¹, (5 Å) 3346.80, 1656.05, 1483.10, 987.04, 539.20, 470.53, 407.16 cm⁻¹). The philosophy for using calcinated zeolites was to allow for the heterolytic cleavage of H₂, which would ultimately acts as a catalyst and presents reactivity towards the siloxane samples.

2.3.5 Silane stock solutions

Stock solutions of the silanes containing an internal standard (dodecane) were prepared for use in the methanation screening process. The solutions were prepared as shown in Table 8 below. Note that these stock solutions were made for five sample reactions at a time.

Table 8. Stock solutions made using the silane reducing reagent, CHCl₃ and dodecane.

Silane Name	Silane Volume/ mL	Moles of silane used per sample/ mol	CHCl ₃ Volume/ mL	dodecane Volume/ mL	Amount of stock solution removed per sample/ mL
diethylsilane	1.1	0.0018	2.0	1.0	0.83
triethylsilane	1.4	0.0018	2.0	1.4	0.95
n-butylsilane	1.1	0.0018	2.0	1.0	0.84
hexylsilane	2.0	0.0025	2.8	2.6	1.5

2.4 Reaction gas mixture composition

The compositions used for the reaction gas mixtures are outlined in Table 9 below.

Table 9. Composition of the gas mixtures used for the methanation reactions.

Experimental Gas used at 15 and 29 psig	
Gas Name	Relative mol% used / %
CO ₂	30
N ₂	25
Ar	20
H ₂	25

Argon was used as an internal standard and N₂ was used as the make-up gas.

2.5 Data Acquisition

For the MS instrument, specific calibrations were conducted in order to ensure the instrument was in optimal working condition and the data collected would be accurate and not prone to any offsets from various conditions including background gas present within the instrument and specific limits of detection towards various ions being considered for analysis. Both instrumental and experimental calibrations needed to be considered prior to any sample analysis. Instrumental calibration approaches involved: gas specific sensitivity, mass scale calibration, QMS offset and zero gas (background) measurement. Calibration of gas specificity sensitivities were used for obtaining calibration factors required for each ion mass considered. The mass scale calibration was used for instrumental troubleshooting to define peaks shapes and alignments across masses selected for analysis. For example, the middle of each peak was directly aligned at the selected ion mass and a sharp peak shape was established. Additionally, QMS offset factors were regularly updated to correct for instrumental drifts. MS experimental calibrations involved collecting respective ion currents for the ion masses selected at the two pressures considered (15 psig and 29 psig).

2.6 Siloxane to Silane reductions

2.6.1 H-Cube Reductions

For H-cube reductions, an H-Cube Continuous-Flow Hydrogenation Reactor (ThalesNano) was used. The experimental setup and sampling techniques are shown in the pictures found in Appendix 3. The parameters and experimental conditions used for the H-cube are outlined in the Table 10.

Table 10. Instrumental parameters and conditions set on the H-cube for reductions.

Details	Value	Units
HPLC Pump	1	mL/ min
Hydrogen Mode	Controlled	-
Hydrogen Pressure	108	bar
Column Heater	50	°C
Pressure Regulator	80	bar
Cartridge Used	10 % Pd/C	-

For the H-cube reductions, the ethoxytrimethylsilane mixtures (0.4 mL) synthesised were diluted in a 1:25 ratio with ethanol (100 %, Unilab, 0.6 mL) in a sample vial.

Before putting the samples through the H-cube, three bed volumes (90 mL in total) worth of ethanol was put through the H-cube system ensuring both cartridge and Teflon wash lines were completely washed of any trace components foreign to the sample. Once the wash was completed, the H₂ cell was initialised and the sample vial was quickly switched with the ethanol wash. A new sample vial was also placed at the end of the H-cube run for product collection. GC-MS runs were performed on the pre and post reduced ethoxytrimethylsilane samples to evaluate any product formation.

2.6.2 Photochemical Reductions

The photochemical reduction system employed a Photolysis Power Lamp Supply (UV Consulting Peschl) connected to the Mercury Vapour Lamp. The experimental design as shown within Appendix 4 was used and involved using two separate reaction systems:

1. Reaction vial (1 mL) with Teflon lined cap. Within the reaction vial was the hexaethylsiloxane stock solution (500 μ L) synthesised using oxalic acid, $5 \times 5 \text{ \AA}$ calcinated zeolites and cyclohexane. The addition of cyclohexane to the reaction vial ultimately acted as an internal standard. Furthermore, the mercury vapour lamp does not break C-C bonds, which have a bond dissociation wavelength of 197 nm, as shown in the spectral distribution of Mercury lamps in Appendix 5. A flea magnet was also placed into the reaction vial for stirring purposes.
2. Reaction vial with the same conditions as above instead containing the hexaethylsiloxane stock solution (500 μ L) synthesised using heptanoic acid.

Both reactions systems had foil-covered H₂ balloons inserted into the Teflon lining using a 22 gauge, 1 1/2" needle. Each of the reaction systems were elevated and set up on either side of the Mercury Vapour Lamp, which was covered in aluminium foil. For the areas where the reaction systems were placed next to the lamp, a window was cut out in the foil to allow

for the direct UV exposure. The reactions were placed onto magnetic stirrers set to a low spin mode ensuring the molecular sieves remain intact. Once the apparatus was set up, the mercury lamp was switched on and covered with a cardboard box for three hours. Pre and post photoreduction reaction solutions were analysed using GC-MS.

2.6.3 Electrochemical Reductions

The electrochemical reduction systems were conducted within a glass cell consisting of a reference electrode, counter electrode and auxiliary electrode all made of platinum. A solution containing the hexaethylidisiloxane synthesised using heptanoic acid (4.380 μL , 0.005000 mol L^{-1}), THF (2.996 mL) and tandem catalyst (5 mol %, 0.0010 g) was placed in the glass cell. A supporting electrolyte tetrabutylammonium perchlorate (Sigma Aldrich Fluka, ≥ 99.0 % for electrochemical purposes, 0.01000 mol, 0.05200 g) was also added to the glass cell. A flea magnet was used for stirring purposes. The electrodes were connected to a Potentiostat (MEP Autolab Potentiostat), which was connected to an e-corder 401 (eDAQ Pty Ltd). The experimental apparatus was placed and operated within a Faraday cage. The parameters were set up for the Potentiostat using GPES (General Purpose Electrochemical System Version 4.9, Eco Chemie B.V.), where the data acquired were also processed and analysed. The specific parameters used are detailed in Table 11.

Table 11. The Potentiostat instrumental parameters and conditions set for the electrochemical reduction system.

Details	Value	Units
<i>Pre-Treatment</i>		
First Conditioning Potential	0	V
Duration	0	s
Equilibrium Time	5	s
<i>Measurement</i>		
Number of Scans	5	-
Cell off after measurement	Yes	-
Standby Potential	0	V
<i>Potentials</i>		
Define start potential w.r.t. OCP	No	-
Start Potential	0	V
First Vertex potential	-3	V
Second Vertex potential	0	V
Step Potential	0.00106	V
Scan Rate	0.1	V/s

The figure below illustrates the glass cell setup as explained above.

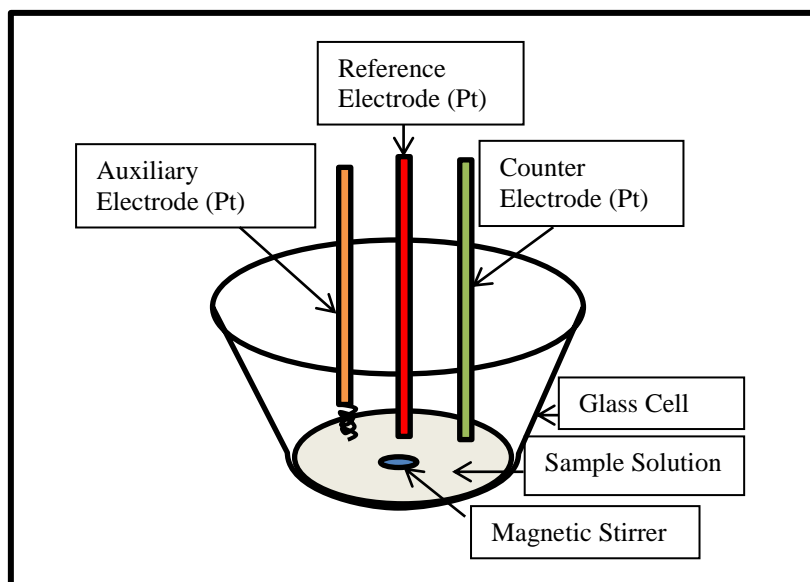


Figure 4. Glass cell experimental setup for electrochemical reduction of siloxanes.

The GPES software was set to acquire the electrochemical reduction data by taking current and potential measurements and presenting the data acquired in the form of a cyclic voltammogram. Measurements were taken for both the sample reaction but also of a blank in THF. The blank solution consisted of all reagents (the same concentrations used as the sample reagent) apart from the hexaethyldisiloxane. Results from the pre and post runs were analysed as both cyclic voltammograms in addition to FTIR analyses.

2.7 Final Flow Chart: Chronological Review of Experimental Approach

The figure below outlines the order in which all experimental methods were performed throughout the project.

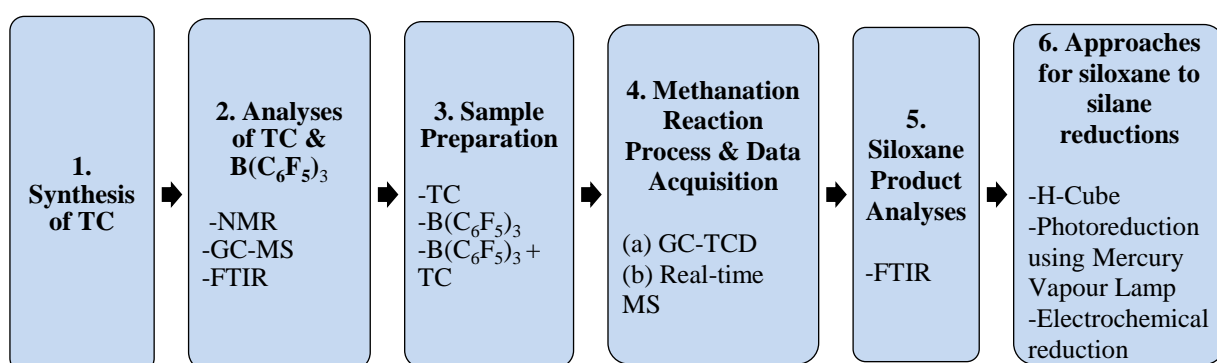


Figure 5. Experimental approach implemented during the project.

Chapter 3: Results and Discussion

3.1 Development of Apparatus

The facilities to undertake small scale pressurised gas/liquid phase reactions were not available at the commencement of this project necessitating the construction of several apparatus needed for the project. These included an apparatus to allow the preparation of quantitative gas mixtures, a reactor system to perform the reactions within and a means of analysing the progress of the reactions in real time. Descriptions of the steps taken and outcomes achieved form the basis of this section.

3.1.1 Production of Quantitative Gas mixtures

At several points in this project there was a need to have quantitative gas mixtures to allow calibration of the various measurement systems used. Initially calibration gas mixtures were ordered through BOC Australia; however the combination of expense, long lead times (4-5 weeks) and relative inflexibility when changes to the mix were needed meant that a more convenient method of calibration gas mixture production was needed.

3.1.1.1 Volumetric gas mixing manifold

The first attempt at producing a gas mixing manifold was to employ the volumetric method of gas mixture production. To that end, a gas mixing manifold, the schematic of which is illustrated in Figure 6, was constructed.

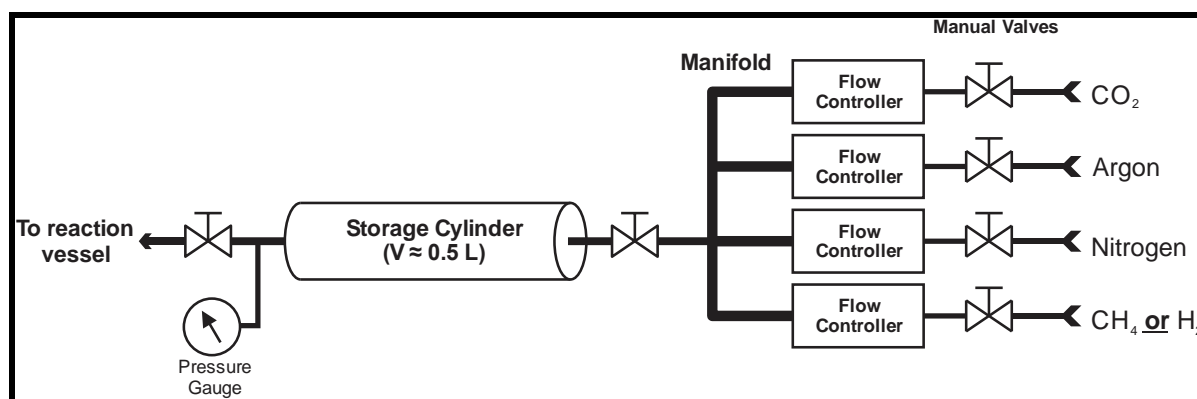


Figure 6. Schematic diagram for the manifold used for the volumetric method of gas mixtures.

Each of the gas lines (CO₂, CH₄, H₂, N₂ and Ar) were supplied at an operating pressure of 400 kPa to the individual Mass Flow Controllers (Brooks 5850 E Series). Each of the mass flow controllers (MFC) were individually calibrated according to the gases they were controlling. Due to the fact that only four existing MFCs were available at the time of construction, one of the MFCs was shared between H₂ and CH₄. The choice of gas in this case

was dependent on whether a calibration mix was being produced (in which case the CH₄ gas line would be connected) or whether a methanation reaction mix was being produced (in which case the H₂ gas line would be connected). The outputs of each MFC were connected in parallel to a ¼ inch stainless steel manifold which ultimately connected through (via a manually operated valve) to a 500 mL acrylic gas storage cylinder (pressure rated to 100 psig).

To prepare a gas mixture, a total flow of 1000 standard cubic centimetres per minute (sccm) was defined as a target flow from the manifold. Each of the individual flow controllers were then set to a flow corresponding to the volumetric fraction of 1000 cm³ required. For example, to prepare a gas mixture at a total pressure of 15 psig (29.70 psia, 2.05 bar) containing 30 mol % CO₂, 20 mol % Ar, 25 mol % CH₄ and 25 mol % N₂, the flow rates of the CO₂, Argon, CH₄ and N₂ MFCs would be set to 200 sccm, 250 sccm, 250 sccm and 250 sccm respectively. To start a fill, the manual valves before and after the storage cylinder were opened and the MFCs were set to the appropriate flows. The combined gas mix from each of the MFCs was allowed to flow through the manifold and storage cylinder for 5 minutes to allow all the flows to stabilise and for the storage cylinder to be flushed. The total gas flow rate exiting the storage cylinder was verified using a ProFlow6000 Electronic Flowmeter (Restek Corporation). Once the flow had stabilised, the manual valve at the exit of the storage cylinder was closed and the pressure allowed to rise to the target pressure (i.e. 15 psig) at which point the manual valve at the head of the storage cylinder was closed and the MFC's stopped.

Several calibration gas mixtures were produced and analysed by GC-TCD and online MS. In both cases non-linear calibrations were obtained with considerable scatter. Initially it was thought that there was inadequate mixing of the produced gas mix in the storage cylinder resulting in a non-homogenous gas mixture. To address this possibility, a magnetic stirrer bean was introduced into the storage cylinder and a magnetic stirrer placed underneath the outside of the storage cylinder to drive the stirrer bean in order to create enough turbulence for the gases to blend. Whilst this approach did appear to improve the scatter, the non-linearity remained. Time constraints did not allow the exact cause of the non-linearity to be established although many possible causes were investigated. Instead, the volumetric method of gas mixture production was abandoned in favour of the partial pressure method.

3.1.1.2 Partial pressure gas mixing manifold

With the problem of non-linearity from the volumetric method of gas mixture production unresolved, the manifold was modified to allow the partial pressure method of gas mixture

production to be performed. The original manifold was modified as detailed in the schematic in Figure 7.

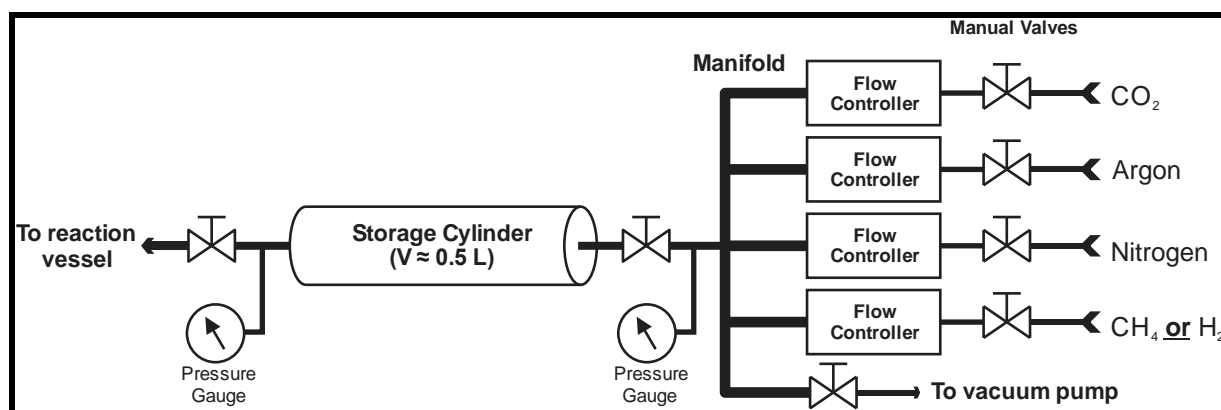


Figure 7. Schematic diagram for the manifold used for the partial pressure method of gas mixture production.

Whilst the MFCs were kept in this design, they were solely used as a means of turning the gas lines on and off as well as a means of controlling the flow rate of each gas as it is introduced into the storage cylinder. A typical gas mixture preparation using this manifold was performed as follows. The system manifold and storage cylinder were first evacuated to less than 0.01 bar (0.15 psia). The first component of the gas mixture was then slowly (to avoid errors from excessive temperature changes) allowed to flow into the empty storage cylinder until the desired pressure was reached. All valves were then closed and a period of 5 minutes was allowed for the storage cylinder to thermally equilibrate before the final pressure recorded. Prior to introduction of the second of the gas mixture, the manifold was again evacuated (to less than 0.01 bar). The second component was then introduced into the manifold until the pressure in the manifold was slightly greater than the pressure in the storage cylinder (to prevent backflow of the filled component). The second component was then slowly allowed to flow into the storage cylinder until the desired pressure is reached. Again, the storage cylinder was allowed to thermally equilibrate before the final pressure reading was recorded. Additional components were introduced into the storage cylinder by repeating the above technique until all components have been added and the final working pressure achieved. The contents of the storage cylinder were mixed by magnetic stirring for 10 minutes before the gas mix was used.

As an example, to prepare a gas mixture at a total pressure of 15 psig (29.70 psia, 2.05 bar) containing 30 mol % CO₂, 20 mol % Ar, 25 mol % H₂ and 25 mol % N₂, the filling proceeded as follows:

The system (manifold and storage cylinder) was evacuated to less than 0.15 psia and this initial pressure recorded as P_{init} . The partial pressure of each of the components in the mixture will be:

$$P_{CO_2} = \frac{30 \times (29.70 - P_{init})}{100} = 8.87 \text{ psia} \quad P_{Ar} = \frac{20 \times (29.70 - P_{init})}{100} = 5.91 \text{ psia}$$

$$P_{H_2} = \frac{25 \times (29.70 - P_{init})}{100} = 7.39 \text{ psia} \quad P_{N_2} = \frac{25 \times (29.70 - P_{init})}{100} = 7.39 \text{ psia}$$

The first component, CO₂ is then slowly introduced into the storage cylinder until a pressure of $(8.87 + P_{init})$ psia is obtained, i.e. 9.02 psia if $P_{init} = 0.15$ psia. The second component is then slowly introduced as describe above until a pressure of $P_{CO_2} + P_{Ar} + P_{init} = 14.93$ psia is reached. This process is continued until all components have been added at which point the final pressure of 29.70 psia will have been reached.

Several calibration gas mixtures were produced and analysed by GC-TCD and online MS. In both cases the calibrations obtained were linear (with R² of better than 0.99). The relative uncertainty for the final concentrations in the produced gas mix was estimated to be $\pm 4.0\%$ based on compressibility factors (which were not considered) and slight changes in temperature over the course of the fill. Consequently, all reaction and gas mixtures used in this study were prepared using this partial pressure method. It should also be noted here that the gas mixtures produced were being referenced to themselves and thus the absolute concentration (i.e. the accuracy) was not considered significant as long as the level of precision was acceptable.

3.1.2 Reactor design

Two designs of reactor vessel were trialed. The first design (Figure 8) utilised a heavy walled glass reaction vial (Reacti-Vial™, Thermo Scientific) fitted with a screw cap made of PTFE which had four Teflon lines through it and were sealed from within the cap.



Figure 8. Reactor Design 1

The lids were screwed onto glass reaction vials containing the sample catalyst and magnetic stirrer. To these vessels the silane stock solutions were added via a Luer lock gas tight syringe and the valve closed. However, once the reaction vessel was pressurised with the experimental gas mixtures (at 15 psig) the vessel was found to leak, albeit slowly. Several attempts were made to quell the leak, however all attempts proved fruitless and this initial design was abandoned in favour of a more robust design.

The second reactor design (Figure 9) employed a metal outer pressure vessel into which a glass reactor vial was placed. The outer pressure vessel was constructed from $\frac{3}{4}$ " copper tube. A 7 cm length of $\frac{3}{4}$ " copper tube was cut and washed, oven dried and cooled to room temperature to remove trace impurities. To one end of the tubing a copper end cap was fitted and silver brazed into position. To the other end of the tube a $\frac{3}{4}$ " Brass Swagelok® Cap (Part No. B-1210-C) was swaged in place. As a separate step, three $\frac{1}{8}$ " holes were drilled into the top of the $\frac{3}{4}$ " Brass Swagelok® Cap equidistance from one another. Inserted into each of the

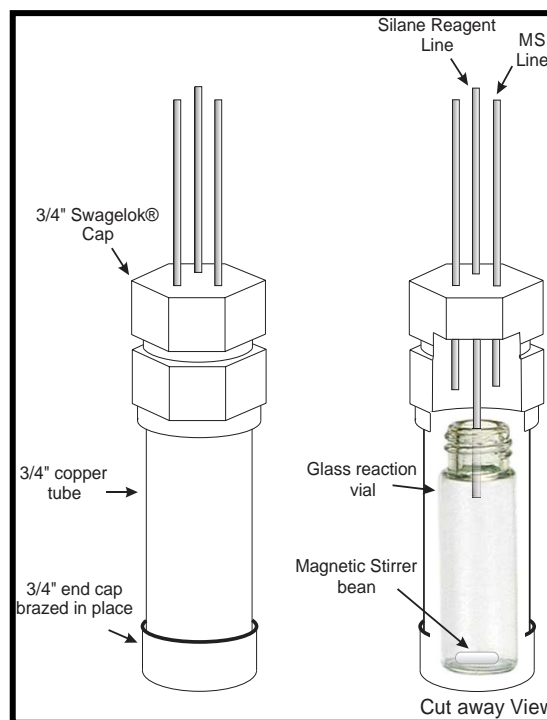


Figure 9. Reactor Design 2

three holes to a depth of 5 cm were 15 cm lengths of $\frac{1}{8}$ " copper tube which were then brazed in place. Next, $\frac{1}{16}$ " PTFE tubing was pushed through two of the $\frac{1}{8}$ " copper tubes until the desired length was achieved and cut. One of the PTFE tubing lengths was intentionally left longer than the other. The longer PTFE tubing was labelled, "Silane Reagent Line" and the other "MS Line". The third line was used to supply the reaction gas mixture and was connected to the gas mixture manifold. The "Silane Reagent Line" was used to introduce reactants into the reaction vial, the extra length on this line was to ensure that the line passed into the glass reaction vial. The $\frac{1}{16}$ " PTFE tubing were sealed to $\frac{1}{8}$ " copper tubes using $\frac{1}{16}$ " to $\frac{1}{8}$ " Swagelok® reducing unions (Part B-200-6-1). On the external facing end of the $\frac{1}{16}$ " PTFE line connected to the silane reagent line, an on/off rotary ball valve (Upchurch) fitted with a female luer lock was connected. Using this line each stock solution sample would be introduced via a Gas tight syringe (SGE, 10 mL, Product #10MDR-LL-GT), which has a removable Luer Lock cap fitting. The line defined as the MS line was connected directly to a 3-port valve switch, which was also connected through to the MS. Using this custom-designed reaction vessel, the methanation reactions were performed and no gas leaks were detected. This yielded an optimised experimental setup allowing both reactions under pressure and for interfacing to a gas analyser for real time analyses of reaction products. Figure 10 illustrates how the reactor was plumbed together.

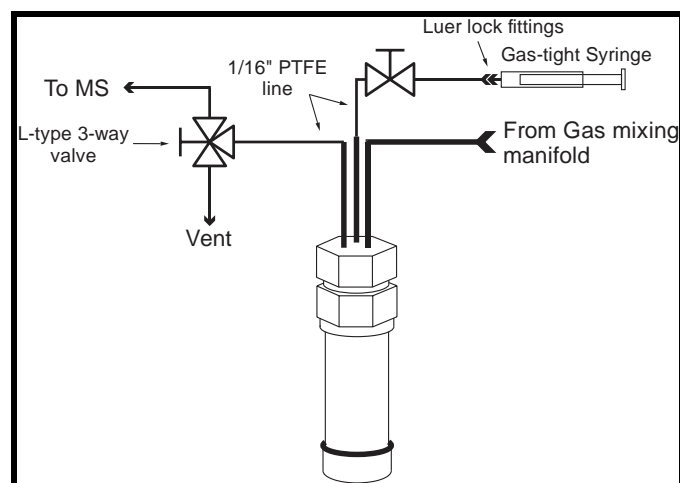


Figure 10. Connections made to the reaction vessel.

During the experimental runs, the specifics of the reaction temperature, residence time and pressure were considered and controlled through various means, especially when kinetic data was to be generated from the reactor experiments. The temperature of the experimental runs were controlled by placing the reactor vessels into heating blocks, which were allowed to thermally equilibrate prior to the injection of the silane stock solutions and release of the gas mixtures. Additionally, the residence time of the experimental runs was controlled using a magnetic stirrer within the gas manifold setup. Specifically when each individual gas component was added to the storage cylinder, the manual valves were sealed and the magnetic stirrer was allowed to mix the gas samples for 3 minutes until the gases were diffused homogeneously. The determination of homogenous diffusion and the time required for complete diffusion was previously investigated through the duration of the project. Lastly, the pressures of the experimental runs were controlled using the ProFlow6000 Electronic Flowmeter (Restek Corporation) in conjunction with the pressure gauges.

3.2 Reaction Product analysis

Two methods of reaction product analysis were employed in this study. The first was a real time system employing a Balzer Prisma QMS-422 Mass Spectrometer Gas Analyser; the second used Gas Chromatography with thermal conductivity detection (GC-TCD).

3.2.1 Online MS

Mass spectrometry (MS) is a technique involving the measurement of the mass to charge (m/z) ratios of various ions within the gas phase²⁴.

As illustrated in Figure 10 the MS was connected directly to the pressurised reactor vessel to allow direct sampling of the head space of the reaction vessel. As this “sampling” results in the continual removal of the head space, which is subsequently replaced by gas flow from the gas mixing manifold, any products from the methanation reaction will be continually diluted. Consequently the concentration of reaction products reported by the MS will appear to decrease (rather than increase) with time. This can be illustrated by examining the real time methane concentration trace, as reported by the MS, , produced from the reaction of diethyl silane/ $B(C_6F_5)_3$ (Sample ID S013, Table 5) with 30 mol% CO_2 at 15 psig (Figure 11); the concentration of methane peaks at about 120 s then begins to gradually decrease until data collection was stopped.

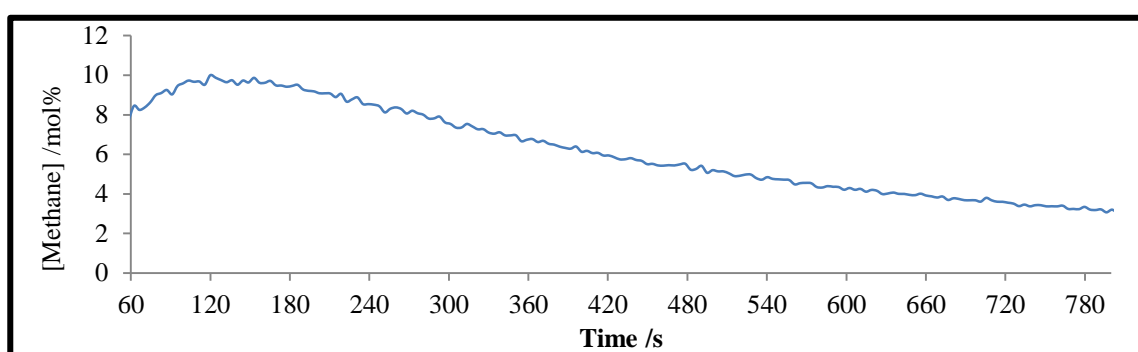


Figure 11. Real time methane concentration trace, as reported by the MS, produced from the reaction of diethyl silane/ $B(C_6F_5)_3$ +TC with 30 mol% CO_2 at 15 psig. Data shown is from 60 s onwards. Prior to 60 s the signal from the MS is unreliable due to fluctuating pressure changes as flows stabilise.

If it is assumed that instantaneous and perfect mixing is occurring between the reaction head-space and the incoming reagent gas and that the headspace is being introduced into the MS at a constant rate, then the concentration seen by the MS can be modelled using a variation of the basic room purge equation, i.e.

$$Conc_{MS} = Conc_{orig} e^{\frac{-Q\tau}{V_r}}$$

Equation 1

where, $Conc_{MS}$ = concentration seen by the MS, $Conc_{orig}$ = concentration prior to dilution, Q = flowrate both into and out of the reaction vessel, τ = time and V_r is the volume of the reactor.

To use this model, both the flow rate into the MS and the volume of the reactor need to be known. The volume of the reactor (V_r) was calculated to be approximately 6.5 cm^3 , however it was not directly possible to measure the flow rate into the MS. So the assumption was made that after 7 minutes (420 s), the reaction being monitored was essentially complete

meaning no further product should be being made and thus the concentration of the product ($Conc_{orig}$) should be constant. By rearranging the equation above to make $Conc_{orig}$ the subject, gives:

$$Conc_{orig} = Conc_{MS} / e^{\frac{-Q\tau}{V_r}}$$

Equation 2

and using $V_r = 6.5 \text{ cm}^3$ and the values for $Conc_{MS}$ and time (τ) taken directly from the MS data, the value for Q was iteratively adjusted until a plot of $Conc_{orig}$ versus time showed no change in $Conc_{orig}$ after 420 s. “No change” was determined by using the linear regression function SLOPE in Excel through data points from 420-480 s. The “Goal Seek” function of Excel was then used to iteratively adjust the value for Q until the SLOPE function returned 0 (or as close to zero as possible). The data from Figure 11 modelled as above is shown in Figure 12 below. In this example, Q was found to be $0.766 \text{ mL min}^{-1}$.

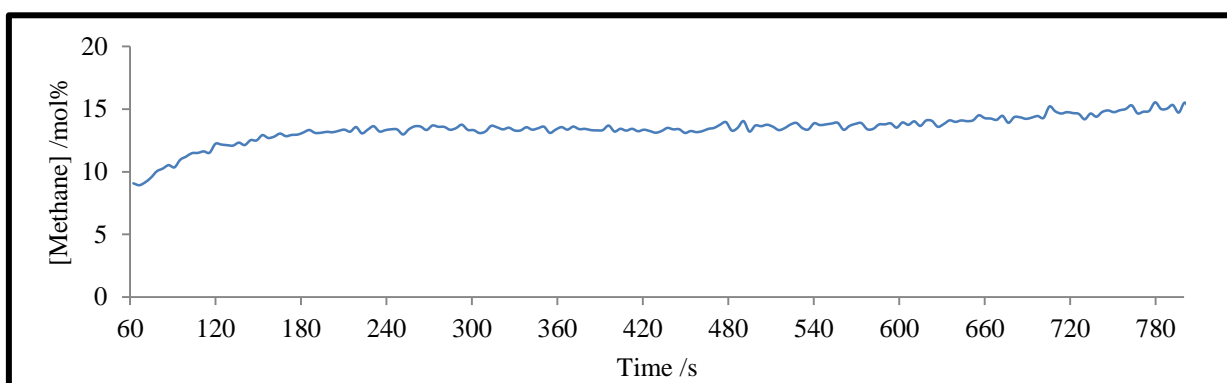


Figure 12. Data from Figure 11 after modelling using Equation 2.

Due to the assumptions made, it is highly likely that the true concentration of the product methane will not be the same as that returned by the model; however the change in concentration with time should still be able to be used to calculate pseudo rate constants for the reaction under study thereby allowing comparison between reagents. The data presented below were all processed using the above technique.

To determine the order of reaction and rate constants for the reaction of CO_2 with the silane/catalyst combinations listed in Tables 5 and 6 the Isolation Method was employed. For a reaction involving two reactants, the rate law for the reaction can be described by the equation $Rate = k[A]^x[B]^y$ where k is the rate constant, $[A]$ and $[B]$ are the concentrations of reagent A and reagent B, and x and y are the reaction orders for reagent A and reagent B respectively. The sum of individual reaction orders, i.e. $x+y$ is known as the overall reaction order. If the concentration of one of the reactants, for example $[B]$, is kept constant during reaction then the term for $[B]$ can be treated as a constant and the rate law becomes: $Rate = k'[A]^x$, where $k' = k[B]^y$. Under these conditions, the observed rate constant, k' , is referred

to as a pseudo-rate-constant. With all reactant concentrations except one essentially constant, simple zero-, first-, and second-order kinetic plots can usually be used to interpret the concentration-time data. In the experiments described below, the concentration of CO₂ is essentially kept constant as a result of both CO₂ being used in a large molar excess over the silane and the fact that any consumed CO₂ is constantly replaced by the “room purge” effect described earlier.

By way of example, the “basic room purge” modelled real time methane concentration trace produced from the reaction of diethyl silane/ B(C₆F₅)₃ + tandem catalyst (Sample ID S009, Table 5) with 30 mol% CO₂ at 15 psig is shown in Figure 13.

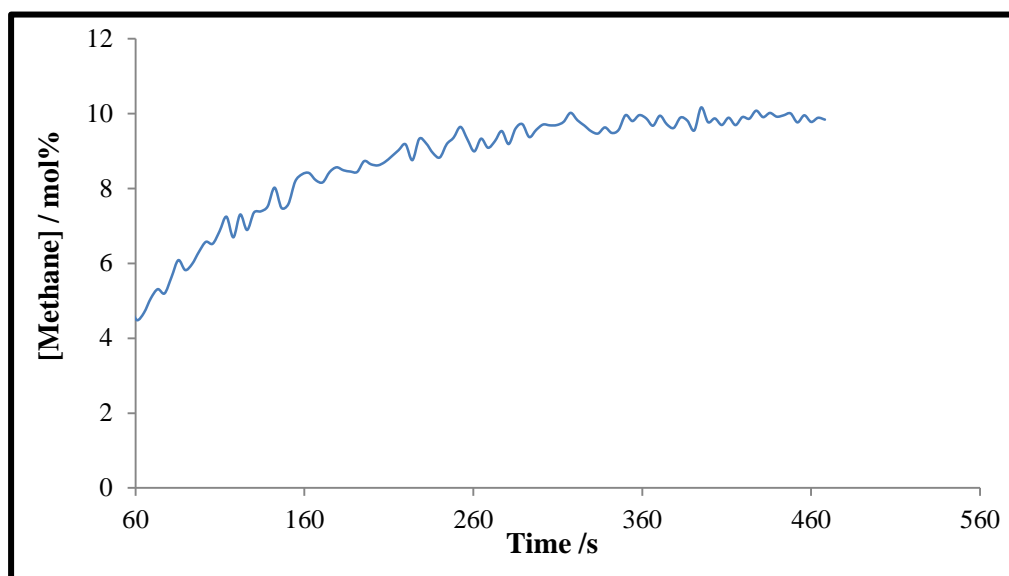


Figure 13. Modelled real time methane concentration trace, as reported by the MS, produced from the reaction of diethyl silane/B(C₆F₅)₃ + tandem catalyst (S009) with 30 mol% CO₂ at 15 psig. The data is shown from 60 s onwards. Prior to 60 s the signal from MS is unreliable due to fluctuating pressure changes as flows stabilise.

As shown, a non-linear relationship is observed between the concentration of methane with respect to time, suggesting the formation of methane is dependent on the concentration of the reactants and thus the reaction is not zero-order. From here further calculations were performed to determine if the reaction was obeying either pseudo first order or pseudo second order kinetics. The real time values for the concentration of methane, as derived from the “basic room purge” model, were defined as “[CH₄]_t” and the maximum concentration of methane was defined as “[CH₄]_{max.}”.

[CH₄]_{max.} for each sample run was determined as the average of the last 8 cycles collected. Using this example, the maximum concentration of methane was determined using the following calculation.

$$[CH_4]_{max.} = \frac{(9.92+9.95+10.0+9.77+9.95+9.78+9.89+9.84)}{8} = 9.89 \text{ mol \% (3 sig. figs)}$$

If the reaction is following pseudo-first-order kinetics, then plotting $\ln([\text{CH}_4]_{\text{max.}} - [\text{CH}_4]_t)$ against time should result in a linear relationship. Additionally, if $1/([\text{CH}_4]_{\text{max.}} - [\text{CH}_4]_t)$ is plotted against time and a linear relationship is observed then the reaction can be said to be following pseudo-second-order kinetics.

Using the example above, the values for the individual experimental methane concentrations were subtracted from $[\text{CH}_4]_{\text{max.}} = 9.89\%$ and the following plots were made.

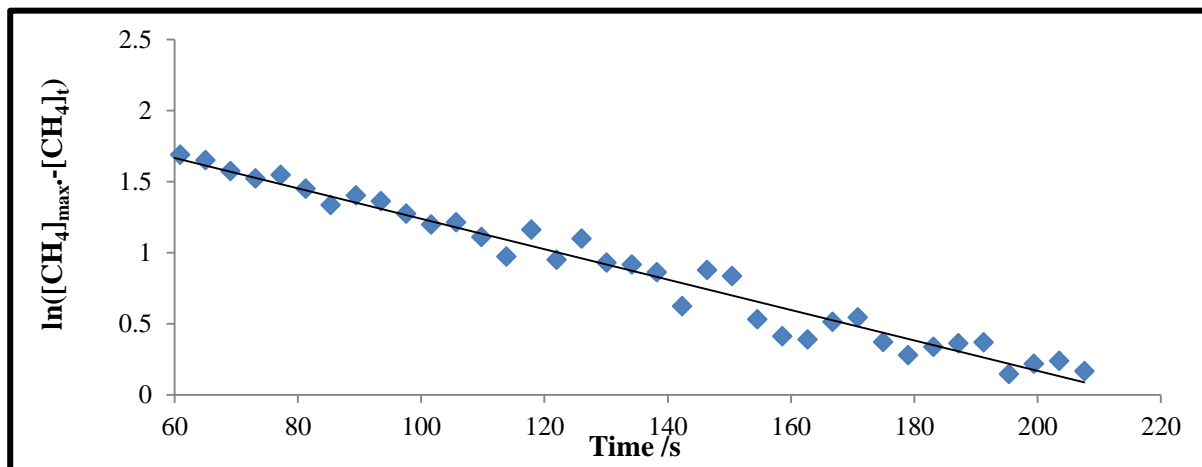


Figure 14. Plot of $\ln([\text{CH}_4]_{\text{max.}} - [\text{CH}_4]_t)$ against time demonstrating a linear relationship between the two parameters, thus establishing a pseudo first order reaction.

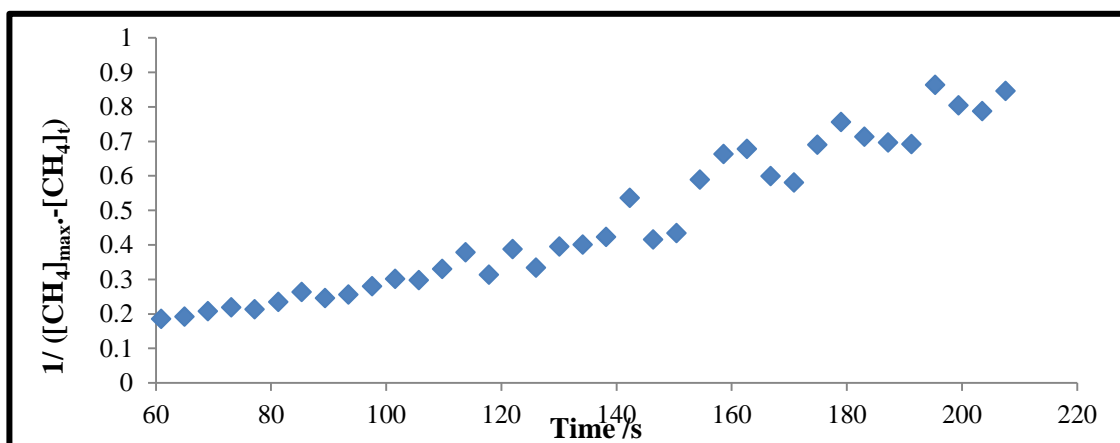


Figure 15. Plot of $1/([\text{CH}_4]_{\text{max.}} - [\text{CH}_4]_t)$ against time demonstrating a non-linear relationship and therefore does not follow a second order reaction.

As shown, a linear relationship is clearly seen between the $\ln([\text{CH}_4]_{\text{max.}} - [\text{CH}_4]_t)$ and time, indicating that the reaction is following pseudo-first order kinetics. Therefore, the pseudo rate constant, k' can be obtained from the slope of the regression line fitting to the data. In this example, the pseudo rate constant was found to be 0.0107 s^{-1} (3 sig. figs). In addition to the rate constant, its 95 % confidence interval can also be determined using the following equation:

$95\% \text{ CI} = t_{0.05,48} \times SE_{\text{slope}}$, where the critical t-value is defined using a statistical table at infinite degrees of freedom (2.01) and SE_{slope} is defined as the standard error of a slope achieved using the LINEST function on Microsoft Excel. Using this example, the 95 % confidence interval is calculated as $2.01 \times 0.000184 = 0.0004$ (1 *sig. fig*). Therefore, the pseudo rate constant for the reaction involving $\text{B}(\text{C}_6\text{F}_5)_3$ + tandem catalyst+ n-butylsilane at 15 psig is $0.0107 \pm 0.0004 \text{ s}^{-1}$. The same calculations were performed for the following reactions as summarised within the table below.

Table 12. A summarised table for calculating the rate constants and respective 95 % confidence intervals for the samples measured at a pressure of 15 psig.

Sample Name	Sample Code	Pseudo 1 st Order Rate Constant / s ⁻¹	95% CI
diethylsilane alone	S017	0.0129	0.0004
TC + diethylsilane	S001	0.00527	0.0007
$\text{B}(\text{C}_6\text{F}_5)_3$ + TC + diethylsilane	S009	0.0107	0.0004
$\text{B}(\text{C}_6\text{F}_5)_3$ + diethylsilane	S013	0.0116	0.0004
TC + triethylsilane	S002	0.00837	0.0006
TC + n-butylsilane	S003	0.0272	0.0003

Unfortunately, data for the remaining sample matrix combinations listed in Table 5 were not able to be obtained due to the unforeseen shutdown of the research laboratories in the Department of Chemistry and Biomolecular Sciences by the University one month before this report was due. However with the data available, the greatest rate constant calculated corresponds to the combination of tandem catalyst and n-butylsilane (S003), determined as $0.0272 \pm 0.0003 \text{ s}^{-1}$. In contrast, the reaction involving the combination of tandem catalyst and diethylsilane yielded the smallest rate constant at $0.00527 \pm 0.0007 \text{ s}^{-1}$. The larger the rate constant obtained from the given calculations, the faster the speed of the reaction. In this case, reactions which have undergone the methanation process at a faster rate will ultimately have greater amounts of methane formed within a defined time frame. Therefore the quickest reaction rate was identified as the one using tandem catalyst and n-butylsilane, suggesting that the greatest yields for methane formation is achieved using a reactive Lewis acid like catalyst with longer chained silanes.

3.2.2 GC-TCD

Gas Chromatography (GC), like all chromatographic systems, is a technique used for the separation of components based on the competitive distribution of those components between a mobile phase and a stationary phase. Components which remain on the stationary phase for

longer periods of time will move slower through the system allow separation based on affinity for the stationary phase²⁴. The GC instrument may also be attached to a thermal conductivity detector (TCD), which is used frequently for gas analyses. The TCD consists of a heated filament, which remains at a constant temperature when there is a constant gas flow of the carrier gas (Helium in this case). However, when compounds with various thermal conductivities pass the filament, the heat is dispersed at various rates causing changes in temperature²⁴.

The use of GC/TCD is a well-established technique for gas analysis. Unfortunately with typical run times of 10 minutes, the use of GC/TCD for real time analysis in this study is not practical as most reactions were complete in less than 3 minutes. That said, GC/TCD is still a useful tool for the analysis of the final gas phase reaction products. The elution order of the expected analytes was determined using standard gas mixes (prepared using the gas mixture manifold described earlier) containing Ar, CH₄, CO₂ and N₂. The chromatogram obtained, however, showed only three peaks, not the four expected. When individual samples of each gas were introduced into the GC, Ar and N₂ were found to co-elute at 2.060 mins. An example of a chromatogram obtained during a sample run is shown in Figure 16 below.

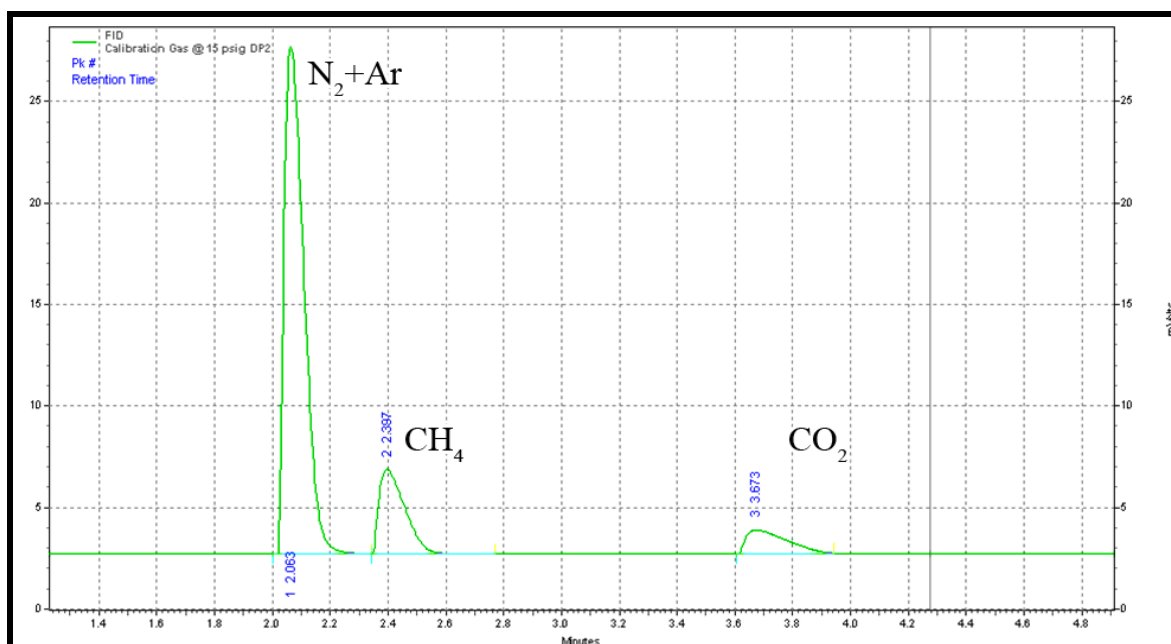


Figure 16. An example of a chromatogram obtained during a sample run using the GC-TCD.

Calibration gas mixtures were produced using the gas mixture manifold and analysed as follows. For the analysis of data achieved using GC, peak area % were used and the calibration plot was drawn (Figure 17), using the Area % of CH₄/Ar multiplied by the relative mol % of Argon (20 %) internal standard injected into the GC.

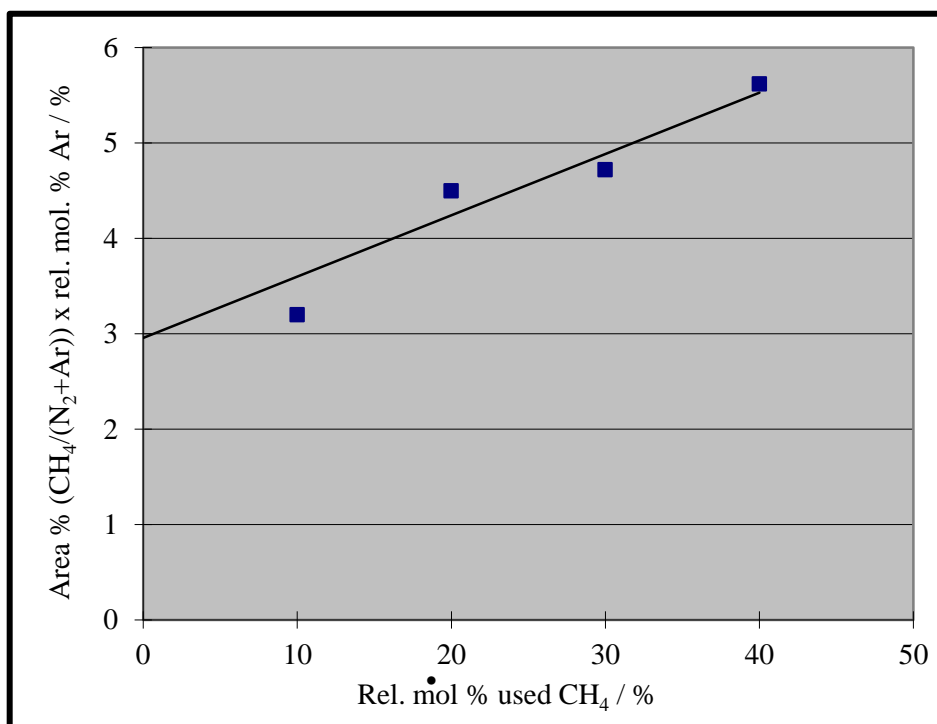


Figure 17. Regression plot for methane calibration showing area % of the methane with respect to the internal standard against the relative percentage of CH₄.

	Value
Slope	0.0607 ± 0.13
Intercept	3.17 ± 4.19

Using the calibration plot, the relative mol % of CH₄ was determined in each of the samples via interpolation/extrapolation. A summary of the parameters collected and an example of the calculations used for quantitation are shown below.

Table 13. The relative mol % of methane calculated at 15 psig using the percentage area of each gas component and interpolating from the regression plot shown in Figure 17.

15 psig		Area %		Absolute relative mol CH ₄ / %
Sample Code	Sample Name	CH ₄	N ₂ + Ar	
S017	diethylsilane alone	1.46	71.4	45.4
S001	TC + diethylsilane	4.05	77.5	35.0
S013	B(C ₆ F ₅) ₃ + diethylsilane	1.56	70.9	44.9
S009	B(C ₆ F ₅) ₃ + TC + diethylsilane	3.58	75.7	36.6
S018	triethylsilane alone	8.55	77.3	15.7
S002	TC + triethylsilane	2.81	74.1	39.7
S014	B(C ₆ F ₅) ₃ + triethylsilane	17.8	79.7	21.3
S010	B(C ₆ F ₅) ₃ + TC + triethylsilane	19.3	78.9	28.4
S019	n-butylsilane alone	19.8	78.0	31.3
S003	TC + n-butylsilane	1.49	81.6	46.1
S015	B(C ₆ F ₅) ₃ + n-butylsilane	24.8	74.1	57.9
S011	B(C ₆ F ₅) ₃ + TC + n-butylsilane	21.3	77.7	38.2
S020	hexylsilane alone	20.6	76.1	37.1

S004	TC + hexylsilane	25.1	71.8	62.8
S016	B(C ₆ F ₅) ₃ + hexylsilane	20.4	75.2	37.2
S012	B(C ₆ F ₅) ₃ + TC + hexylsilane	16.9	78.1	19.0

Table 14. The relative mol % of methane calculated at 29 psig using the percentage area of each gas component and interpolating from the regression plot shown in Figure 17.

29 psig		Area %		Absolute relative mol CH ₄ / %
Sample Code	Sample Name	CH ₄	N ₂ + Ar	
Si05	diethylsilane alone	13.5	75.9	50.9
S025	B(C ₆ F ₅) ₃ + diethylsilane	15.9	74.1	42.5
Si06	triethylsilane alone	15.3	76.8	45.8
S022	TC + triethylsilane	16.1	72.5	40.7
S026	B(C ₆ F ₅) ₃ + triethylsilane	16.1	73.5	41.4
Si07	n-butylsilane alone	11.6	74.7	56.1
S023	TC + n-butylsilane	1.38	85.6	87.8
S027	B(C ₆ F ₅) ₃ + n-butylsilane	11.7	74.5	55.6
Si08	hexylsilane alone	12.9	73.8	51.4
S024	TC + hexylsilane	20.2	69.7	25.3
S028	B(C ₆ F ₅) ₃ + hexylsilane	16.5	73.0	40.0

An example calculation to determine the relative mol % of CH₄ used was for the TC + diethylsilane sample (sample code S001) as shown below.

$$\text{Area \%} \left(\frac{\text{CH}_4}{(\text{N}_2 + \text{Ar})} \right) \times \text{rel. mol \% Ar} = \text{slope} \times \text{rel. mol \% CH}_4 + \text{intercept}$$

$$\therefore 1.044 = 0.0607 \times \text{rel. mol \% CH}_4 + 3.17$$

$$\therefore \text{rel. mol \% CH}_4 = 35.0 \% \text{ (3 sig. figs)}$$

The same calculations were repeated for all samples and summarised in the table above.

As mentioned previously, all samples analysed by GC-TCD were taken from the reactor headspace after approximately about 10 minutes into the run. Therefore, all relative mol % CH₄ calculations can be compared as time is a constant factor.

As shown, the reactions at lower pressures (15 psig) using the tandem catalyst with the silanes presented the greatest relative mol % of CH₄ produced. In contrast, at higher pressures (29 psig) the reactions with only silane stock solutions involved (that is with no catalysts) presented the greatest relative mol % of CH₄ produced. Furthermore, when comparing both pressure systems to one another, the average mol % of CH₄ produced is most significant when using n-butylsilane as a reducing reagent, with averages of 43.3 % at 15 psig and 39.0 % at 29 psig. As the data surprisingly suggests, reactions processed at higher pressures technically do

not require the use of catalysts (either the $B(C_6F_5)_3$ or tandem catalyst) as the silane stock solutions manage to push the reaction forward obtaining relatively higher yields of CH_4 over time. This can be explained as the Si-H bonds are weakened even further when under pressure. It is already well known that the Si-H bond can be easily dissociated due to the properties of hydrogen in both its bonding and antibonding states. When comparing hydrogen in its antibonding sites to its bonding sites, the Si-H bond length is ~3 % longer and has a 1.3 eV greater energy than its counterpart²⁵. Due to these properties and the environment in which the Si-H bond is placed in, the Si-H bond is defected and hydrogen becomes trapped within its antibonding site. Therefore, due to differences in energy gaps created, the Si-H bond becomes dissociated²⁵. This may be the case for longer chained primary silanes (such as n-butylsilane), however this does not apply with secondary and tertiary silane reagents (such as triethylsilane), which are hindered by steric factors. Furthermore when bulky compounds such as $B(C_6F_5)_3$ or the tandem catalyst are incorporated at higher pressures, the direct interaction between the silane reagents and the experimental gas mixtures are reduced overall, leading to lower yields for the formation of CH_4 . This however does not seem to be the case when considering the use of the tandem catalyst and n-butylsilane at higher pressures which yielded the highest level of CH_4 formation overall (87.8 %). This suggests Lewis acid type catalysts used in conjunction with a long chained silane reducing reagents provide optimum amounts of CH_4 formed.

However, due to limited catalyst available, only single sample runs could be performed for the analysis of CH_4 formation via the methanation process. In order to gain greater confidence in these conclusions, this experimental would need to be repeated.

Table 15 provides a summary comparing results obtained between the data acquired using real-time MS and the GC-TCD.

Table 15. Comparison of the calculated rate constants and percentage yield of CH_4 determined at 15 psig using real-time MS and GC-TCD measurements.

Sample Name	Sample Code	Rate Constant / s^{-1}	CH_4 yield / mol%
diethylsilane alone	S017	0.0129	45
TC + diethylsilane	S001	0.00527	35
$B(C_6F_5)_3$ + TC + diethylsilane	S009	0.0107	37
$B(C_6F_5)_3$ + diethylsilane	S013	0.0116	45
TC + triethylsilane	S002	0.00837	40
TC + n-butylsilane	S003	0.0272	46

As shown, there is a clear correlation between the rate constant of the reaction and the relative yield of CH₄ produced. That is, the greater the value calculated for the rate constant, the greater the relative percentage of CH₄ produced (in 10 minutes). At both low and high pressures, the incorporation of the tandem catalyst as well as n-butylsilane proves most efficacious; achieving highest yields of CH₄ formed. However, there is a slight difference between yields when utilising the tandem catalyst to those using silanes alone. This is ultimately more appealing to commercial industries as it could save expenses required for purchasing and synthesising tandem catalysts.

3.2.3 FTIR

FTIR spectroscopy is a particularly important technique which is used in various branches of chemistry to gain both qualitative and quantitative information. It is a method utilised from which identification of certain functional groups within compounds can be determined.

IR spectra were acquired for the reaction samples which had undergone the methanation process. In confirmation to the production of siloxane byproducts, comparisons were drawn between samples using the same silane stock solutions against the different catalysts and pressures considered. For example, when considering the samples using n-butylsilane at 15 psig (S019, S003, S015 and S011), the spectra demonstrate differences in relative proportions of silanes being consumed and siloxanes formed. The information obtained from this can be compared to reactions using n-butylsilane at 29 psig (Si07, S023 and S027). The spectra for each reaction set performed are shown in Figure 18.

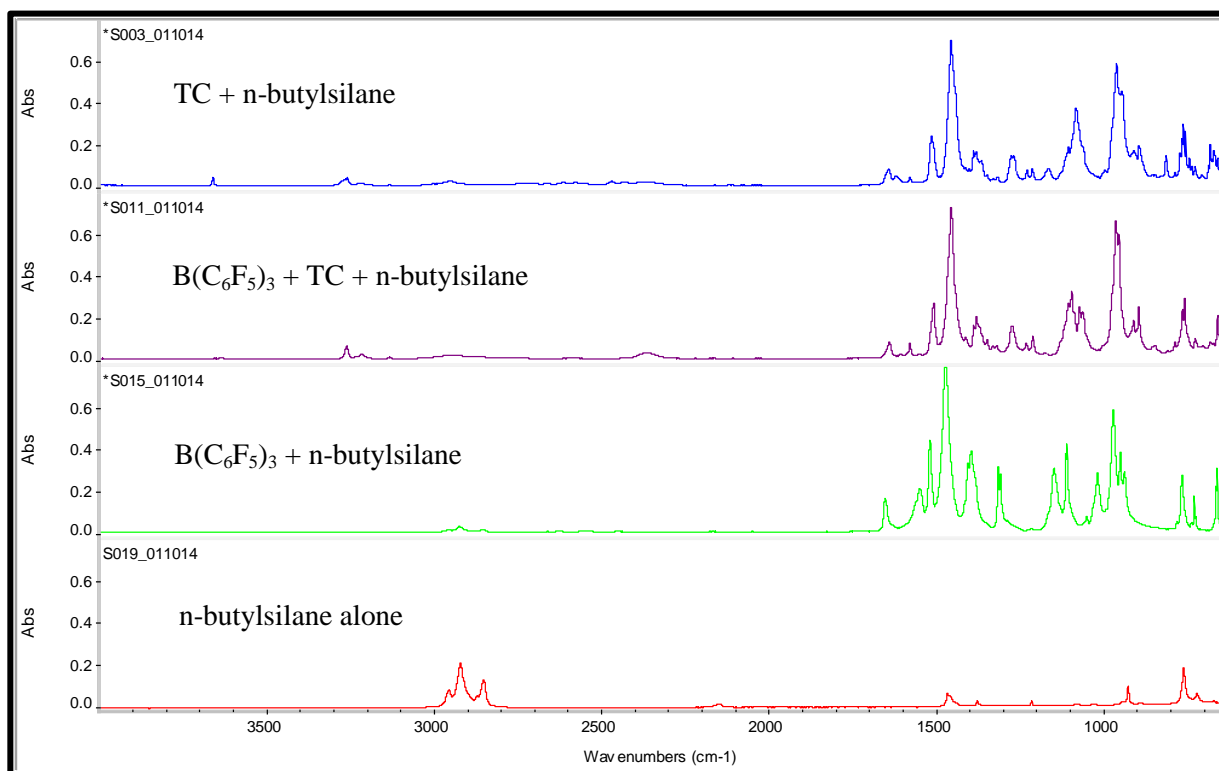


Figure 18. Stacked IR spectra of reaction samples using n-butylsilane at 15 psig.

The sharp peak at 1455.75 cm^{-1} across all samples that contain one form of catalyst is a characteristic peak for C-F stretching mode. Additionally, the strong peaks at $954.60\text{-}968.31\text{ cm}^{-1}$ are representative of the =C-F bending mode of the catalytic moiety. The weak and sharp peak found in both the TC + n-butylsilane and TC + $\text{B}(\text{C}_6\text{F}_5)_3$ + n-butylsilane at 3261.93 cm^{-1} is characteristic of the N-H stretching mode of the amine functional group identified on the structure of the tandem catalyst. The strong and broad peaks at $2852.98\text{-}2956.72\text{ cm}^{-1}$ are characteristic of the C-H stretch found in alkanes. Also, a small yet sharp peak is observable at 2150.88 cm^{-1} reflecting the presence of the Si-H stretching mode still found within the sample reaction after it had undergone the methanation process. This would suggest that the relative yield of methane formed would be lower when compared to its counterparts. Most importantly, the peaks shown between $1000\text{-}1100\text{ cm}^{-1}$ are all associated to the Si-O-Si stretching mode found in the siloxane byproducts obtained.

Similarly, the stacked spectra of the sample reactions which had undergone the methanation process using n-butylsilane at 29 psig provides similar information to that at 15 psig, but still presents with a couple differences. Firstly, a strong and sharp peak is observable at 757.43 cm^{-1} being characteristically associated to the C-Cl stretching mode found in chloroform. This signal is also visible in the 15 psig spectra, however is overridden by the catalyst stretching mode. The fact that the same peak is minimal in the 29 psig run suggests

that the catalyst had been used to completion within the methanation processes conducted at relatively higher pressures. Similarly, the Si-O-Si stretching mode is also found between 1000-1100 cm^{-1} , confirming the formation of siloxanes. The information obtained from the spectra act as the first level of confirmation for the conversion of silanes to siloxanes. As an extension, this would also suggest the formation of methane, which has already been established in the MS and GC-TCD analyses.

3.3 Regeneration of Silane: Evaluation of Siloxane to Silane Reduction Strategies.

As illustrated in the previous section, the use of silanes for the reduction of CO_2 to methane is efficient and requires only mild conditions. However for silane based methanation to be useful for widespread CO_2 conversion, a mechanism must be in place to allow the conversion of the siloxane byproducts of the methanation reaction back to silanes so that the process can be continued. Ideally this conversion should use readily available resources such as hydrogen and solar energy. The following sections detail some very preliminary attempts at achieving siloxane to silane conversion.

3.3.1 Reduction over metal catalysts

The conventional method of reduction over Group 8 metals such as palladium and nickel was evaluated as a means of siloxane to silane conversion. Although, as stated in the introduction, such reductions can and have been used directly for CO_2 to methane conversion, it was trialled here as a “proof of concept” exploration. The hydrogenation reaction was undertaken using an H-Cube® Continuous-flow Hydrogenation Reactor (ThalesNano, Inc.). The H-Cube® was chosen for this exploratory study as the continuous flow regime employed by the device would be ideally suited to continuous regeneration of silane in a practical CO_2 to methane plant. The H-Cube® operates using a continuous-flow of substrate, in this case siloxanes, combined with hydrogen, which is generated in-situ from the electrolysis of water.

The Hydrogen/Substrate mixture can be heated and pressurized up to 100°C (212°F) and 100 bar (1450 psi) respectively, however the conditions listed in section 2.5.1 were used. The mixture is then passed through a packed catalyst cartridge where the reaction takes place and the product continuously elutes out of reactor and into a collection vial.

A simple model siloxane, ethoxytrimethylsilane was chosen for this exploratory study. The assumption being that if this simple siloxane could not be reduced, then more complicated siloxanes such as those produced from the CO_2 methanation would also not be

able to be reduced. The reaction was monitored by GC-MS where the substrate solution was compared before and after the H-Cube® runs were performed. Figure 20 depicts the chromatograms of the substrate before and after reduction.



Figure 19. GC-MS chromatograms of the pre and post H-cube reductions depicting no new peaks being observed.

As shown, the peaks between pre and post H-cube reductions correlate and no new peaks were observed indicating siloxane reduction did not occur. Time constraints did not permit optimisation of the H-Cube conditions so it is not clear if the reduction failed outright or due to non-ideal reaction conditions. For instance, the catalyst cartridge used was 10 % Pd/C which has been shown to have less catalytic activity than say, Raney nickel²⁶. That said, the bond dissociation energy for the Si-O bond is 452 kJ mol^{-1} , which is approximately 1.5 times stronger than the equivalent C-O bond. Thus, some sort of mechanism to weaken/activate the Si-O bond towards reduction may be ultimately necessary to achieve successful reduction.

3.3.2 Photochemical Reductions

In an attempt to weaken/activate the Si-O bond towards reduction, the use of short wavelength UV light to encourage bond dissociation was explored. The short wavelength UV light was supplied via a high powered low pressure mercury vapour lamp. The experimental setup was thought of as an extension to the unsuccessful H-cube reduction. Since the dissociation energy required to break the Si-O bond is relatively high and the Pd/C catalyst did not influence any reduction, the testing of a more active metal-based catalyst deposited on a porous solid matrix (Nickel on Zeolite) was employed. The catalyst was formed by calcinating nickel acetate on zeolites (see Section 2.3.5). It was hoped that the use of zeolites would increase the catalytic surface area allowing better interaction with the “weakened” siloxanes, resulting from exposure to the short wavelength UV radiation. Such theory is justified by a very current study conducted by Segatelli et al. (2014)²⁷. This particular study involved the use of nickel acetate to promote the formation of porous polymer derived

ceramics using poly(dimethylsiloxane). The study showed that with the implementation of the active nickel acetate metal catalyst, the formation of nanowires made up of a composite of silicon, carbon and oxygen were derived. When the nickel acetate was not included as part of the reaction, the production of nanowires was not observed²⁷.

Additionally, the incorporation of zeolites as a solid matrix on which the reduction of the siloxanes could occur would also be ideal for any future directions the project may follow. This includes the incorporation of a solid based matrix as part of the methanation process, where silanes would stick onto the surface of the zeolites, be utilised in the methanation process forming siloxane byproducts which would still be bound to the zeolite surface. These siloxanes could then be reduced into the silane reagents and re-used within the process. Figure 21 shows the GC/MS chromatograms of the pre and post photoreduction samples for the hexadiethylsiloxane.



Figure 20. Chromatogram with stacked peaks for pre and post photoreduction samples using the hexadiethylsiloxanes synthesised with heptanoic acid.

As shown, the peaks between pre and post photoreduction reductions correlate and no new peaks were observed indicating once again that siloxane reduction did not occur. These results further highlight the strength of the Si-O bond and demonstrate just how challenging a one-step reduction of siloxanes to silanes may ultimately be.

3.3.3 Electrochemical Reductions

The failure of two differing attempts to reduce siloxanes by direct metal catalysed hydrogenation does not preclude the possibility that some combination of reaction conditions may yet result in successful reduction. However, with time constraints limiting the permutations and combinations that could be explored, a different approach was attempted through the use of electrochemical means to reduce the siloxanes. The use of cyclic

voltammetry, which provides qualitative data for determining differences between pre and post electrochemical reactions involving the hexaethyldisiloxane was employed. Cyclic voltammetry functions by applying a both a forward and reverse linear potential scan of a stationary working electrode in a cyclic manner. A potentiostat measures the respective current values taken at various time points across the potential scan ²⁸. The information is then translated in the form of a cyclic voltammogram, which plots current vs. potential. A representative cyclic voltammogram plots the response of a single reversible redox reaction in a single cycle, assuming the sample is initially present within its oxidised state. For this reason, the first half cycle operates under a negative potential, until the potential window for the reduction of the sample is reached. At this point, the directional sweep potential is reversed ²⁸.

The idea behind utilising electrochemical methods for the reduction of siloxanes can be attributed to the transfer of electrons from one species to another. In this case, the transfer of electrons via the loss of oxygen and gain of hydrogen can be defined as undergoing reduction, which is the case when regarding the formation of silane from siloxane. Therefore when referring to the acquired data, the forward scan is what needs to be compared and considered when determining variations between pre and post electrochemical runs. The data acquired in the form of cyclic voltammograms are shown in the figures 22 and 23 below.

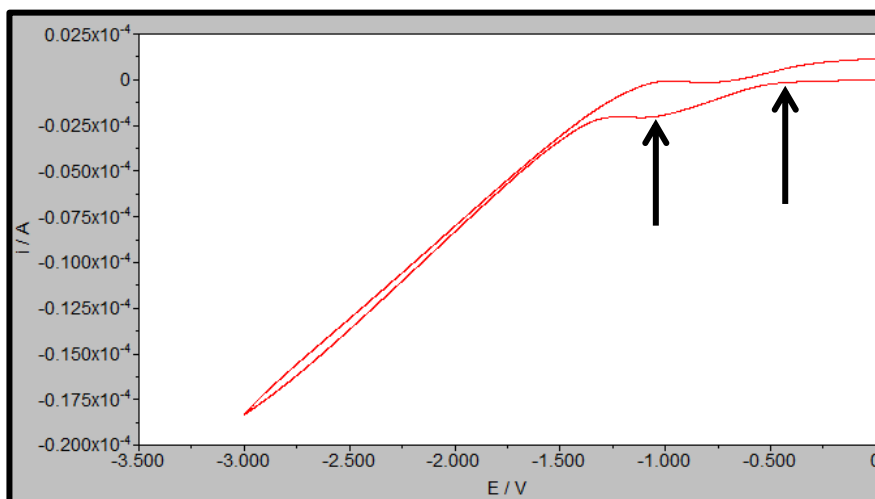


Figure 21. Cyclic voltammogram of a blank sample solution containing THF, tandem catalyst and tetrabutylammonium perchlorate (supporting electrolyte).

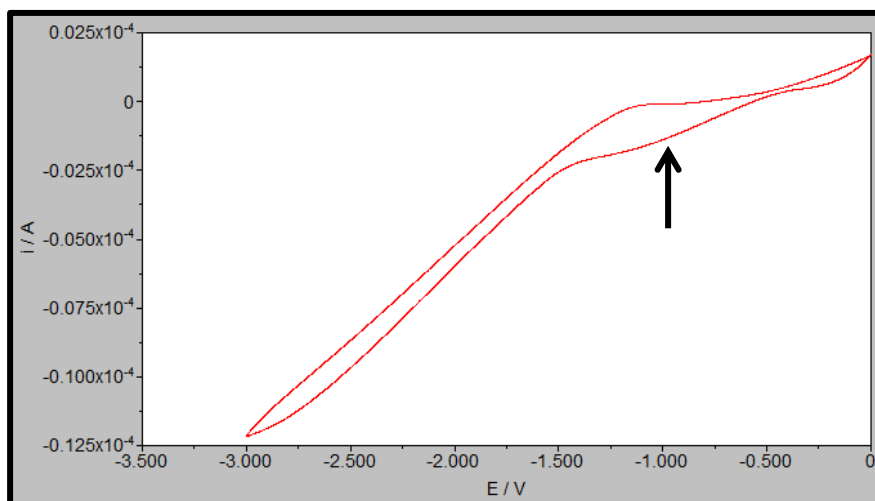


Figure 22. Cyclic voltammogram of a reaction sample solution containing THF, tandem catalyst and tetrabutylammonium perchlorate (supporting electrolyte) and the hexaethyldisiloxane synthesised using heptanoic acid.

Within the cyclic voltammograms, black arrows were used to indicate the differences observed between the blank and reaction samples. From observation, the forward reactions present differences across the potentials of -0.50 V to -1.00 V suggesting that the sample species introduced is being reduced to a completely different product compared to that of the blank sample. This is further confirmed by looking at the cathodic and anodic peak potentials. The cathodic peak potentials for the blank and sample reactions were approximately determined as -1.09 V and -1.18 V respectively. Additionally, the anodic peak potentials for the blank and sample reactions were approximately determined as -1.02 V and -1.23 V respectively. The results from the cyclic voltammograms demonstrate a change within the electrochemical behaviour of the reaction sample which is not identical to the blank sample.

To determine whether there were any structural changes to the hexaethyldisiloxane, further analysis of the pre and post electrochemical reduction samples were completed using FTIR (ATR). By doing so, we would ideally expect to see the Si-O-Si bending and stretching modes diminish and observe new peaks such as the Si-H stretching modes. Figure 24 below presents stacked spectra of the pre and post electrochemical reductions.

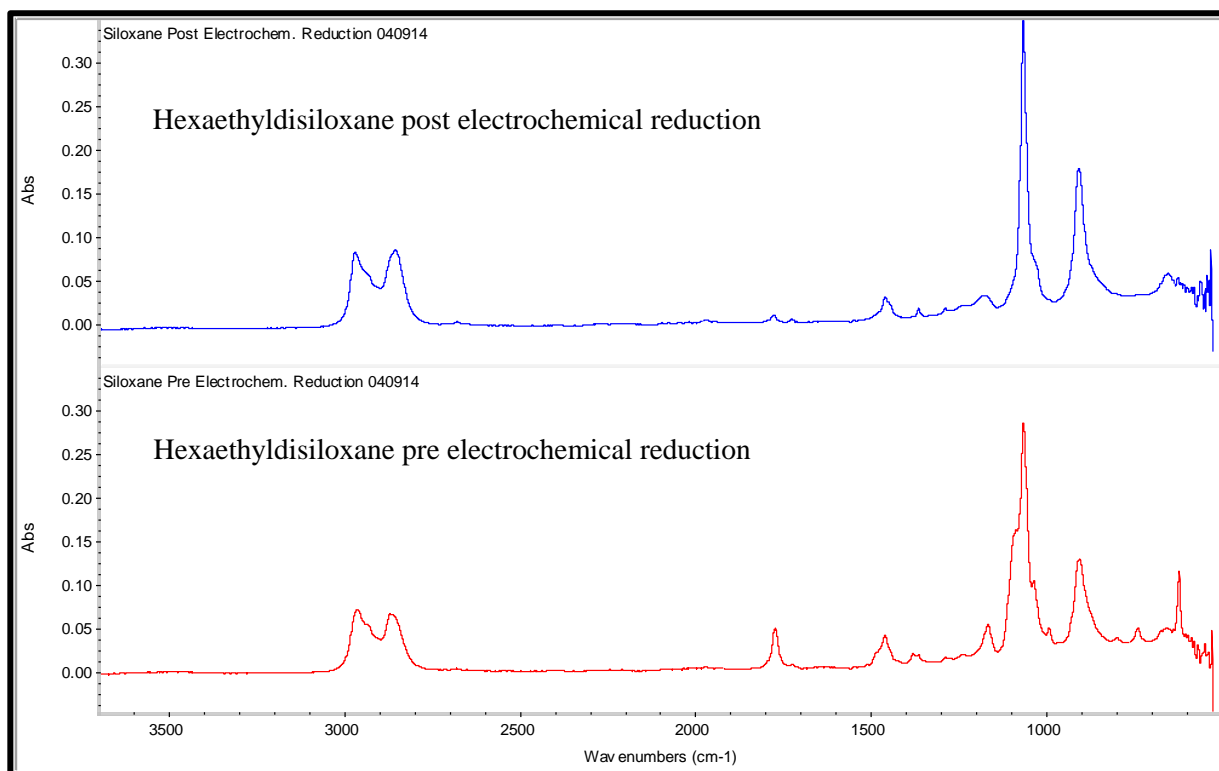


Figure 23. Stacked IR spectra of the pre and post electrochemical reductions.

As shown, the strong sharp peak in the stacked spectra at 1065.34 cm^{-1} is characteristic of the Si-O-Si stretching mode found in the hexaethyldisiloxane. The broad and medium signal peaks remaining unchanged at 2873.39 and 2966.06 cm^{-1} is also characteristic of the C-H stretching mode of the THF solvent. Similarly, the major peaks remaining unchanged at $906.40\text{--}907.40\text{ cm}^{-1}$ is determined as the stretching vibration of the alkyl groups from THF. The peak at 1774.50 cm^{-1} present on the pre electrochemical reduction is representative of the C=O stretching mode found in trace amounts of heptanoic acid remaining from the synthesis of the hexaethyldisiloxane. This peak is substantially diminished in its absorbance as shown in the post electrochemical reduction, suggesting the reduction of heptanoic acid to heptane. This is confirmed by the peaks that start to appear in the post electrochemical run at $1718.34\text{--}1787.69\text{ cm}^{-1}$. Furthermore, degradation of the tandem catalyst is observed with the peak at 1460.77 cm^{-1} which is the C-H bending and also the C-C stretching modes. Weak peaks are observable in the pre electrochemical scan at around 1400 , 1000 and 739.16 cm^{-1} , which is not observed in the post reduction scan. This suggests the presence and reduction of polysiloxane groups present within the sample. This is also confirmed by the strong peak at 622.79 cm^{-1} . This particular result contributes further to the results obtained from the cyclic voltammograms. However, in order to confirm these results, the electrochemical procedure

needs to be repeated for validation. Additionally, the sharp increase in the peak at 1065.34 cm^{-1} is observable and characteristic of the Si-O-Si stretching mode.

Therefore, the combination of data analysed from both the cyclic voltammograms and the IR spectra suggest that no major reduction of siloxanes were determined through the use of electrochemical techniques. Instead, carboxylic acids including heptanoic acid are reduced to their alkane form in addition to breaking bonds between polysiloxane chains.

3.4 Future Directions

It would be interesting to see the effects of other forms of the tandem catalyst synthesised on the overall production of methane. That is, using amines other than 2,2,6,6-tetramethylpiperidine which are both more or less bulky. By doing so, this may alter the activity of the tandem catalyst which would lead to faster or slower rates of reaction for the production of methane.

Secondly, more investigations need to be performed to reduce siloxanes to silanes as part of a one-step reaction. Current methods to achieve this involve converting siloxanes to chlorosilanes which are then reduced using harsh reagents including LiAlH_4 ²⁹. These reactions not only use extremely reactive reducing agents, but also only work under harsh experimental conditions including high temperatures and pressures. For such reasons industries do not reduce siloxanes formed through non-methanation processes, but rather dispose of them using separating systems such as the Applied Filter Technology (SAGTM)¹⁸. This particular form of separation consists of customised adsorbent beds made of activated charcoal and graphitic materials. However, the adsorption of the siloxanes to these materials has still not reached optimum quantities. Furthermore, these adsorbents are not regenerative and generally disposed of, meaning the siloxanes are ultimately released into the environment further contributing to the current accumulation of siloxanes in landfill and the atmosphere¹⁸.

Some possible methods that can be utilised for these reduction systems include:

- Immobilising the siloxanes onto molecular sieves/zeolites reducing them to silanes with ease. A prerequisite for the successful application of silane based methanation of CO_2 is the successful regeneration of the silane reductant. Isolating the siloxane by-products from the reaction mix to be passed on to regeneration poses one of the challenges for silane regeneration. A possible isolation strategy could be attempted via the use of molecular sieve entrapment. Ideally, the siloxanes would bind onto the surface of the molecular sieves in which case one form of reduction may be used for the process to take effect.

- Weakening the siloxane bonds using techniques such as ultrasonication. Throughout the last couple of decades extensive research has been conducted into the effects of ultrasonication. The principle behind sonochemistry uses sound energy to distort and weaken bonds within compounds. Taking advantage of this method could be potentially useful where these weakened bonds could be then suppressed to a source of hydride forming the silane reagent.

In regards to the results achieved within the project, further research is required in fully understanding the reasons as to why the incorporation of the tandem catalyst + n-butylsilane provides relatively higher yields for the production of methane. For this, further kinetic studies could be performed to determine which component is significant when considering concentrations of reagents within this process.

As a future endeavour, the conversion of CO₂ to longer hydrocarbons via the silane/boron-based catalytic activation reaction will also be explored, where the selectivity and reactivity of the system will need to be optimised against the experimental parameters and conditions used.

Chapter 4: Conclusions

This project consisted of three major aims including: (a) development of a custom designed experimental setup to investigate small scale methanation reactions (b) screening a wide range of silane-based reducing reagents against three different forms of catalysts including $B(C_6F_5)_3$, the synthesised tandem catalyst and $B(C_6F_5)_3$ +tandem catalyst to determine the efficiencies and rates of reaction for the formation of CH_4 and (c) determining the effect of the tandem catalyst within the methanation process.

From the results achieved within the project, the custom design of an experimental apparatus was successfully constructed and was implemented as the platform for the methanation reactions to take place. The screening of the reaction samples was successfully achieved and the data recorded utilised techniques including real-time MS and GC-TCD for quantitation. The identification of siloxane byproducts were made using FTIR techniques, where functional groups for the Si-O-Si stretching mode ($1000-1100\text{ cm}^{-1}$) were identified. Additionally, most of the reaction samples showed no observable peaks for the Si-H bending mode ($2100-2360\text{ cm}^{-1}$) suggesting the methanation reaction had gone to completion.

From the quantitative analyses, the overall reaction, which provided relatively highest yields was the tandem catalyst + n-butylsilane reaction suggesting that the use of a protonated Lewis acid catalyst may push the methanation reaction forward to completion. It could also suggest that the use of a long-chained reducing reagent is spatially and stereochemically favourable for the conversion of CO_2 to CH_4 . However, further research is required into confirming the rate determining reagent within the process, which at this point suggests is the silane.

However, when looking at the quantitative analysis from the GC-TCD alone, the greatest yields achieved for CH_4 production showed that no catalysts were essentially required for methanation reactions under higher pressures (29 psig). From a practical point of view, the elimination of a reagent in any reaction has cost and ease of applications benefits.

The regeneration of siloxane byproducts to silane reducing reagents was also investigated within the project, showing no immediate signs of reduction. However, further investigations can be carried out via immobilisation of siloxanes onto zeolites and weakening bonds using sonochemical techniques. The project can even be further expanded by considering production of longer hydrocarbons chains, which would be particularly useful in many applications including chemical storage, cooking, manufacturing and automotive industries.

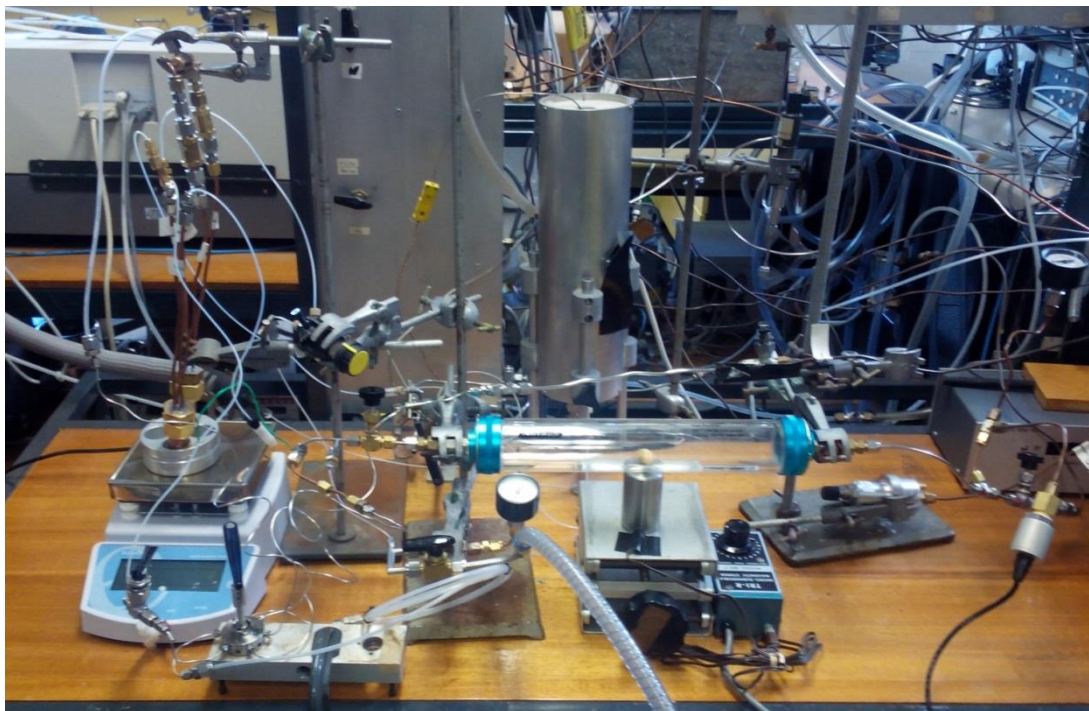
References

- (1) Olivier, J. G. J.; Muntean, M.; Maenhout, G. *Trends in global CO₂ emissions: 2013 Report*; PBL Netherlands Environmental Assessment Agency: Netherlands, 2013; pp 4-7.
- (2) D'Alessandro, D. M.; Smit, B.; Long, J. R., Carbon dioxide capture: prospects for new materials. *Angew Chem Int Ed Engl* **2010**, *49* (35), 6058-6082.
- (3) Tavares, M. T.; Alstrup, I.; Bernardo, C. A. A., Coking and decoking during methanation and methane decomposition on Ni-Cu supported catalysts. *Materials and Corrosion* **1999**, *50*, 681-685.
- (4) Scholten, S. A.; Allison, J. D.; Dunn, B. C. Methanation reaction methods utilising enhanced catalytic formulations and methods of preparing enhanced methanation catalysts. . 2012.
- (5) Sigma-Aldrich Molecular Sieves: AL-143 Mineral Adsorbents, Filter Agents and Drying Agents <http://www.sigmaaldrich.com/chemistry/chemical-synthesis/learning-center/technical-bulletins/al-1430/molecular-sieves.html> (accessed 18/09/2014).
- (6) Meerbeek, A. V.; Jelli, A.; Fripiat, J. J., Reduction of the surface of silica gel by hydrogen spillover. *Journal of Catalysis* **1977**, *46* (3), 320-325.
- (7) Bradford, M. C. J.; Vannice, M. A., CO₂ Reforming of CH₄. *Catalysis Reviews* **1999**, *41* (1), 1-42.
- (8) Ashley, A. E.; Thompson, A. L.; O'Hare, D., Homogeneous hydrogenation of CO₂ to CH₃OH. *Angewandte Chemie* **2009**, *48*, 9839-9843.
- (9) Kondratenko, E. V.; Mul, G.; Baltrusaitis, J.; Larrazabal, G. O.; Perez-Ramirez, J., Status and perspectives of CO₂ conversion into fuels and chemicals by catalytic, photocatalytic and electrocatalytic processes. *Energy & Environmental Science* **2013**, *6* (11), 3112-3135.
- (10) Gurav, J. L.; Jung, I.-K.; Park, H.-H.; Kang, E. S.; Nadargi, D. Y., Silica aerogel: Synthesis and Applications. *Journal of Nanomaterials* **2010**, *2010*, 11.
- (11) Larson, G. L.; Halides, M., Silicon-based Reducing Agents. In *Silicon, Germanium & Tin Compounds, Metal Alkoxides and Metal Diketonates*, Inc., G., Ed. Pennsylvania, U.S.A, 2008; pp 127-130.
- (12) Sumerin, V.; Schulz, F.; Nieger, M.; Leskelä, M.; Repo, T.; Rieger, B., Facile heterolytic H₂ activation by amines and B(C₆F₅)₃. *Angewandte Chemie International Edition* **2008**, *47* (32), 6001-6003.
- (13) Sumerin, V. Lewis Acid-Lewis Base Mediated Metal-Free Hydrogen Activation and Catalytic Hydrogenation. Academic Dissertation, University of Helsinki, Finland, 2011.
- (14) Stephan, D. W., "Frustrated Lewis pairs": a concept for new reactivity and catalysis. *Organic & biomolecular chemistry* **2008**, *6* (9), 1535-9.
- (15) Nimmagadda, R. D.; McRae, C., A novel reduction of polycarboxylic acids into their corresponding alkanes using n-butylsilane or diethylsilane as the reducing agent. *Tetrahedron Letters* **2006**, *47* (21), 3505-3508.
- (16) Ishihara, K.; Hanaki, N.; Funahashi, M.; Miyata, M.; Yamamoto, H., Tris(pentafluorophenyl)boron as an Efficient, Air Stable, and Water Tolerant Lewis Acid Catalyst. *Bulletin-Chemical Society of Japan* **1995**, *68*, 1721-1730.
- (17) Inc., X. A., Treatment Solutions for Landfill Gas Fuel Applications. 2007; pp 2-4.
- (18) Ajhar, M.; Travesset, M.; Yuce, S.; Melin, T., Siloxane removal from landfill and digester gas - a technology overview. *Bioresource technology* **2010**, *101* (9), 2913-23.
- (19) Launer, P. J. *Infrared Analysis of Organosilicon Compounds: Spectra-Structure Correlations* Laboratory for Materials Inc. : Burnt Hills, New York, 12027, 1987; pp 100-103.

- (20) Nimmagadda, R. D.; McRae, C., Characterisation of the backbone structures of several fulvic acids using a novel selective chemical reduction method. *Organic Geochemistry* **2007**, *38* (7), 1061-1072.
- (21) Fulmer, G. R.; Miller, A. J. M.; Sherdan, N. H.; Gottlieb, H. E.; Nudelman, A.; Stoltz, B. M.; Bercaw, J. E.; Goldberg, K. I., NMR Chemical Shifts of Trace Impurities: Common Laboratory Solvents, Organics, and Gases in Deuterated Solvents Relevant to the Organometallic Chemist. *Organometallics* **2010**, *29*, 2176-2179.
- (22) Herold, D. A.; Futrell, J. H., Unimolecular Decomposition of Ethoxytrimethylsilane. *Organic Mass Spectrometry* **1989**, *24*, 984-988.
- (23) Schenk, U.; Hunger, M.; Weitkamp, J., Characterisation of basic guest compounds on solid catalysts by ^{13}C CP/MAS NMR spectroscopy of surface methoxy groups. *Magnetic Resonance in Chemistry* **1999**, *37*, S75-S78.
- (24) Kitson, F. G.; Larsen, B. S.; McEwen, C. N., *Gas Chromatography and Mass Spectrometry: A Practical Guide*. Academic Press: U.S.A, 1996.
- (25) Tuttle, B.; Walle, C. G. V. d., Structure, energetics, and vibrational properties of Si-H bond dissociation in silicon. *Physical Review B* **1999**, *59* (20), 12884-12889.
- (26) Huber, G. W.; Shabaker, J. W.; Dumesic, J. A., Raney Ni-Sn Catalyst for H_2 Production from Biomass-Derived Hydrocarbons. *Science* **2003**, *300* (5628), 2075-2077.
- (27) Segatelli, M. G.; Kaneko, M. L. Q. A.; Silva, V. P.; Yoshida, I. V. P., Porous Ceramic Materials from Polysiloxane-Clay Composites. *Journal of the Brazilian Chemical Society* **2014**, *25* (4), 716-725.
- (28) Wang, J., *Analytical Electrochemistry (Third Edition)*. John Wiley & Sons Inc. : Hoboken, New Jersey & Canada 2006.
- (29) Preparation of Reactive Functional Groups on PET surfaces. In *Polymer Brushes: Substrates, Technologies, and Properties*, Illustrated ed.; Mittal, V., Ed. CRC Press Taylor & Francis Group: New York, 2012; p 93.
- (30) Davidson, M. W. Education in Microscopy and Digital Imaging. <http://zeiss-campus.magnet.fsu.edu/articles/lightsources/mercuryarc.html>.

Appendix

Appendix 1: Methanation Experimental Setup



Appendix 2: Gas cylinder with magnetic stirrer placed underneath, in addition to a magnetic heating block.



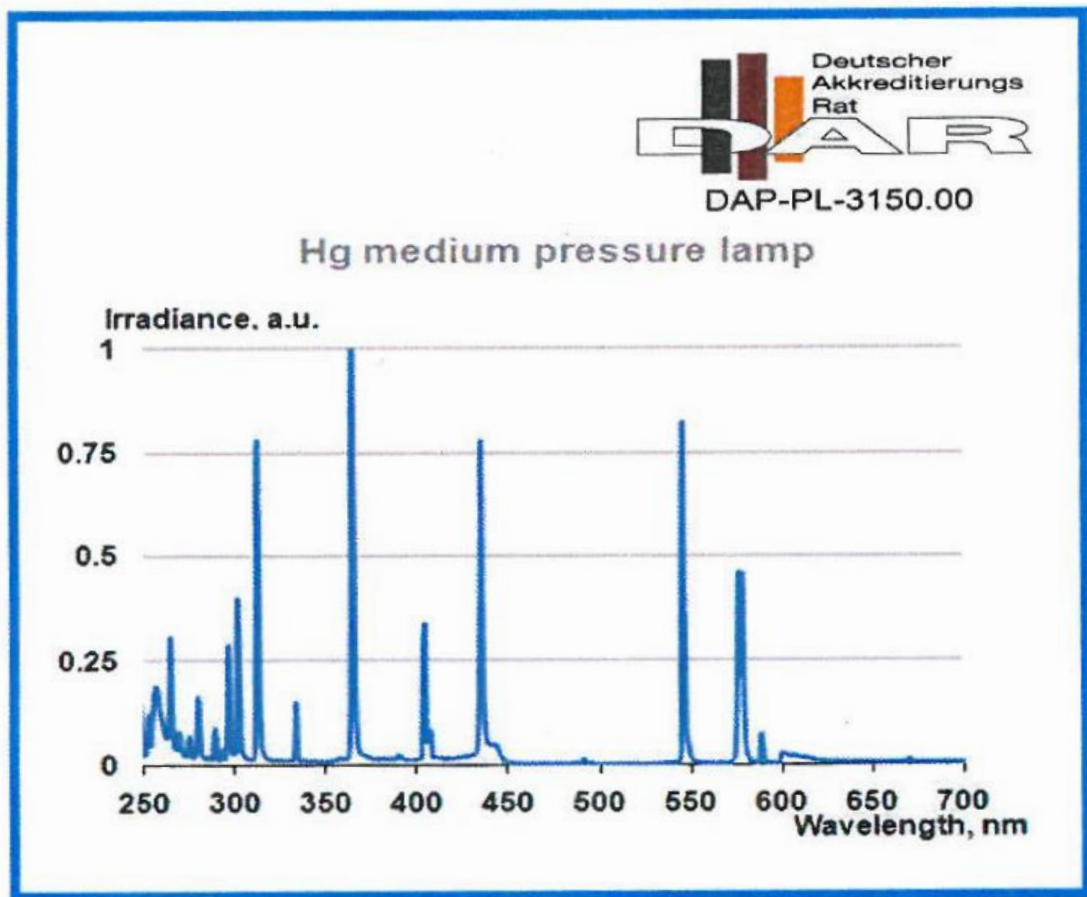
Appendix 3: H-Cube experimental setup, reaction and product sample vial positioning.



Appendix 4: Photoreduction experimental setup using the Mercury Vapour Lamp, foil-covered H₂ (g) balloons and the sample reaction vials with the molecular sieves.



Appendix 5: Spectral Distribution of Mercury Lamps³⁰



Appendix 6: Experimental sample matrices used for real-time MS and GC-TCD data acquisition for both 15.00 and 29.00 psig.

Pressures = 3 atm. ~ 29.00 psig Direct Measurement MS				
S#	Silane / μL	Silane Used	CHCl_3/ mL	dodecane (int. std.)/ μL
Si05	227.8	diethylsilane	0.4	206.9
Si06	280.9	triethylsilane	0.4	273.0
Si07	228.2	n-butylsilane	0.4	206.9
Si08	283.6	hexylsilane	0.4	378.2

S#	TC / mg	TC used / mg	Silane / μL	Silane Used	CHCl_3/ mL	dodecane (int. std.)/ μL
S021	64.00	61.1	227.8	diethylsilane	0.4	206.9
S022	64.00	62.8	280.9	triethylsilane	0.4	273.0
S023	64.00	62.5	228.2	n-butylsilane	0.4	206.9
S024	64.00	65.1	283.6	hexylsilane	0.4	378.2

S#	$\text{B}(\text{C}_6\text{F}_5)_3$ / mg	$\text{B}(\text{C}_6\text{F}_5)_3$ used / mg	Silane / μL	Silane Used	CHCl_3/ mL	dodecane (int. std.)/ μL
S025	50.00	51.1	227.8	diethylsilane	0.4	206.9
S026	50.00	50.5	280.9	triethylsilane	0.4	273.0
S027	50.00	52.2	228.2	n-butylsilane	0.4	206.9
S028	50.00	48.6	283.6	hexylsilane	0.4	378.2

Pressures = 2 atm. ~ 15.00 psig Direct Measurement MS				
S#	Silane / μL	Silane Used	CHCl_3/ mL	dodecane (int. std.)/ μL
S017	227.8	diethylsilane	0.4	206.9
S018	280.9	triethylsilane	0.4	273.0
S019	228.2	n-butylsilane	0.4	206.9
S020	283.6	hexylsilane	0.4	378.2

S#	TC / mg	TC used / mg	Silane / μL	Silane Used	CHCl_3/ mL	dodecane (int. std.)/ μL
S001	64.00	62.8	227.8	diethylsilane	0.4	206.9
S002	64.00	62.5	280.9	triethylsilane	0.4	273.0
S003	64.00	64.1	228.2	n-butylsilane	0.4	206.9
S004	64.00	64.7	283.6	hexylsilane	0.4	378.2

S#	$\text{B}(\text{C}_6\text{F}_5)_3$ / mg	$\text{B}(\text{C}_6\text{F}_5)_3$ used / mg	Silane / μL	Silane Used	CHCl_3/ mL	dodecane (int. std.)/ μL
S013	50.00	49.3	227.8	diethylsilane	0.4	206.9
S014	50.00	51.4	280.9	triethylsilane	0.4	273.0
S015	50.00	48.2	228.2	n-butylsilane	0.4	206.9
S016	50.00	50.3	283.6	hexylsilane	0.4	378.2

S#	$\text{B}(\text{C}_6\text{F}_5)_3$ / mg	$\text{B}(\text{C}_6\text{F}_5)_3$ used / mg	TC / mg	TC used / mg	Silane / μL	Silane Used	CHCl_3/ mL	dodecane (int. std.)/ μL
S009	25.00	22.4	32.00	30.8	227.8	diethylsilane	0.4	206.9
S010	25.00	23.8	32.00	30.4	280.9	triethylsilane	0.4	273.0
S011	25.00	26.6	32.00	30.2	228.2	n-butylsilane	0.4	206.9
S012	25.00	32.3	32.00	30.1	283.6	hexylsilane	0.4	378.2